Tools for Assessment and Planning of Aquaculture Sustainability

SHORT TITLE:	**TAPAS**
COORDINATOR:	**Prof. Trevor Telfer**
ORGANISATION:	**University of STIRLING, UK**
TOPIC:	**H2020- SFS-11b-2015**
PROJECT NUMBER:	**678396**

DELIVERABLE: 6.6

Earth Observation and model-derived aquaculture indicators report

Public

Contributing Authors:

Stephanie Palmer, Laurent Barillé, Pierre Gernez ; UN
Stefano Ciavatta, Hayley Evers-King, Susan Kay, Andrey Kurekin, Benjamin Loveday, Peter I. Miller, Stefan Simis, Robert Wilson; PML
Kostas Tsiaras; HCMR
Phil Wallhead, Trond Kristiansen, André Staalstrøm, Trine Dale, Richard Bellerby; NIVA

History of changes:

Ver	Date	Changes	Author
1	27/08/2019	Initial draft template	SP
2	27/09/2019	All contributions included for each section	All
3	04/10/2019	Full draft for comments and changes	SP
4	21/10/2019	Full draft for internal review	All

Internal review

Date	Name
30/10/2019	Trevor Telfer (UOS)

This project has received funding from the EU H2020 research and innovation programme under Grant Agreement No 678396

Refer to this document as:

Palmer, S., Barillé, L., Gernez, P., Ciavatta, S., Evers-King, H., Kay, S., Kurekin, A., Loveday, B., Miller, P.I., Simis, S., Wilson, R., Tsiaras, K., Wallhead, P., Kristiansen, T., Staalstrøm, A., Dale, T., Bellerby R., 2019. Earth Observation and model-derived aquaculture indicators report. TAPAS project Deliverable 6.6 report. 65 pp.

This project has received funding from the EU H2020 research and innovation programme under Grant Agreement No 678396

SUMMARY

Space available for aquaculture, in Europe as elsewhere, is in limited supply and high demand. Additional tools are required to support the identification of potential new sites and to assess their suitability and sustainability for various aquaculture segments. In this report, various aquaculture indicators that were derived using satellite Earth Observation and modelling approaches as part of *Tools for Assessment and Planning of Aquaculture Sustainability* (*TAPAS*) are presented. These cover far-field, regional ecosystem-scale coastal and offshore aquaculture segments in different parts of Europe. Indicators specific to shellfish and finfish biology and farms are presented, as are more general biogeochemical indicators, and include the identification of current and forecasted future opportunities for aquaculture, as well as environmental risks to the industry.

Specifically, satellite ocean-colour observations are used to produce maps of optical water types and suspended particulate matter extremes for the North East Atlantic and Mediterranean, and of harmful algal bloom risk in north-western European waters for the current period (Section 2; PML). Output from a 3D hydrodynamic-biogeochemical ocean model (POLCOMS-ERSEM) is used to produce indicators of current (early-century) and future (mid- and late-century) aquaculture suitability for the Mediterranean Sea and the North West European shelf sea, notably water temperature, phytoplankton and zooplankton biomass, and degree day modelled maps of Pacific oyster spawning and metamorphosis potential, under different climate scenarios (Representative Concentration Pathways 4.5 and 8.5; Section 3; PML). Section 3 output is used in further pan-European modelling of Pacific oyster growth potential via dynamic energy budget (DEB) theory, transformed into industry-relevant indicators for the early- and late-century scenarios (Section 4; UN). The evaluation of Mediterranean finfish Aquaculture Allocated Zone carrying capacity, through the modelling of near-surface currents, chlorophyll-a, and dissolved inorganic nutrients used to calculate environmental indicators and an overall environmental index, also made use of Section 3 outputs (Section 5; HCMR). Additional 3D hydrodynamic-biogeochemical ocean modelling (A20) outputs have been used for macro-siting of offshore salmon and mussel aquaculture in the North Atlantic and Nordic Seas, using thresholds of several output variables to establish and map environmental suitability indices for each (Section 6; NIVA).

The compiled approaches and proposed indicators are relevant to diverse European aquaculture segments and situations, and could be individually selected or mix-and-matched to best respond to the particular context or question. Using far-field models, large-scale zones of interest are highlighted for broad aquaculture planning and policy development, which can be then considered in higher resolution at subsequent planning and decision-making steps. Long-term sustainability and uncertainties were considered through the implementation of various climate and management scenarios in modelled forecasting of indicators. Such consideration of different scenarios helps zones of interest to be identified, and also serves to highlight which factors are expected have the greatest impact on the given aquaculture sector.

This project has received funding from the EU H2020 research and innovation programme under Grant Agreement No 678396

TABLE OF CONTENTS

This project has received funding from the EU H2020 research and innovation programme under Grant Agreement No 678396

1. Introduction

Both population and per capita seafood consumption are projected to continue to increase in Europe, as elsewhere (FAO, 2018). Europe is already one of the largest consumers of seafood globally, but imports supply more than 60% of EU seafood consumption (STECF, 2018), leaving it vulnerable to international dynamics. On the global scale, aquaculture is currently on par with fisheries contributions to seafood production, with the latter stagnating and the former on the rise (Fig.1.1; FAO, 2018). In Europe, however, despite declines in capture fisheries, aquaculture only contributes approximately 20% of seafood production (STECF, 2018) and this proportion is growing at a much slower rate than aquaculture production worldwide; very few new farming licences have been issued in more than a decade (Hofherr et al., 2015). The top two hindrances to aquaculture expansion in Europe have been cited as being lack of available space in the coastal zone and lack of coherent priorities and management (Hofherr et al., 2015).

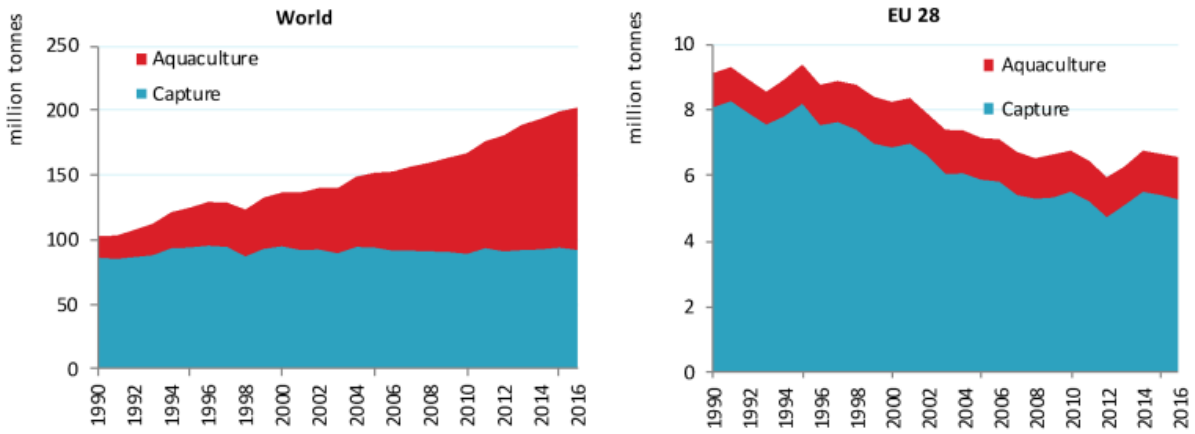

Figure 1.1. "World and EU28 seafood production (capture and aquaculture): 1996-2016. Data source: FAO, 2018". From STECF (2018).

Several advantages to expanding aquaculture further offshore have been identified, in addition to fewer space constraints and use conflicts typically encountered there. These include less exposure to anthropogenic pollutants, enhanced production and carrying capacity, and less acute impacts on the environment compared with near-coastal cultivation, and coincide with technological advances that at least partially overcome or compensate for some challenges associated with offshore, open-water conditions (Holm et al., 2017). Adequate spatial planning in the offshore as in the nearshore environment remains crucial to the sustainable development of the aquaculture industry. Regulators and decision makers can circumvent negative perceptions and use conflicts that have been known to plague aquaculture by proposing allocated zones for aquaculture, within which companies can assess the suitability of and select sites based on their foreseen production (Sanchez-Jerez et al., 2016). Such long-term and comprehensive planning can benefit from the use of full-coverage spatial data over large areas, such as that only possible to obtain through Earth Observation and modelling (Meaden et al., 2013).

This project has received funding from the EU H2020 research and innovation programme under Grant Agreement No 678396

Future climate change and related uncertainties further complicate the identification of and planning for sustainable aquaculture, whether at existing or new sites. Changes to many of the biogeochemical variables crucial to many marine aquaculture sectors are projected to be dramatic, including to water temperature, productivity, acidification, freshwater inputs, and dissolved oxygen concentrations, but to be highly variable over space and depending on the climate model and emissions scenario (IPCC, 2019; FAO, 2018). Generally, mariculture potential is expected to decline substantially by the end of the century under a "business-as-usual" scenario (IPCC, 2019). Biogeochemical model projections can be made under various climate change scenarios and for various future time periods, and thereby provide a range of possible aquaculture outcomes to assess the sensitivity of different sectors in different regions.

Here, several approaches to transforming rich spatiotemporal datasets from EO, hydrodynamic-biogeochemical modelling, and shellfish growth modelling into tangible aquaculture indicators for use in pan-European and long-term planning and policy development are presented for shellfish and fin-fish aquaculture. These are accompanied by specific examples and interpretation, but provide a flexible framework that regulators and decision makers can adapt and combine to best inform the specific challenges and questions they face. The uncertainties related to ongoing climate change facing the aquaculture industry and all of society are considered by producing indicators under different future climate scenarios. While there are many climate models and potential emissions scenarios, those chosen here demonstrate an approach to spatially assessing the sensitivity of various aquaculture segments to climate change; other scenarios could foreseeably be applied as desired. Broad areas of interest, in terms of their current potential and stability under changing climate scenarios, have been highlighted using the approaches presented here. Such far-field approaches are therefore expected to be of particular interest in prioritizing or establishing allocated zones for aquaculture at the international (i.e., European), national, or regional scales over the long-term, within which more detailed investigation of site-level suitability could be undertaken, for example using the complementary near-field approaches developed in *TAPAS* Work Package 5 (Falconer et al., 2019).

This project has received funding from the EU
H2020 research and innovation programme
under Grant Agreement No 678396

2. Assessing current suitability for aquaculture across Europe based on satellite observation

2.1 Introduction

This section presents only indicators of current aquaculture suitability in European seas, derived from ocean colour satellite observations. In particular, we present maps of optical water types (Section 2.2), of suspended particulate matter extremes (Section 2.3) and of risk of harmful algal blooms (Section 2.4). The indicators derived from satellite observations do not represent all conditions and indicators of water quality that will affect aquaculture suitability.

2.2. Optical water type indicator

Coastal waters cover a wide range of optically-complex conditions, from clear blue open ocean, to harmful coastal blooms and sediment plumes. Conditions are typically highly dynamic in both spatial and temporal dimensions. This diversity of conditions precludes the adoption of single algorithms to retrieve in-water concentrations (for example, of total suspended sediment (TSM) and chlorophyll (CHL)). To reduce the complexity of this problem, we have applied an optical water typing approach to European coastal waters (Moore et al., 2014). In contrast to previous approaches using *in situ* data (Spyrakos et al., 2018), our approach is based on using remotely-sensed observations to derive the representative spectra indicative of a given optical water type (OWT). This approach is similar to that used by the European Space Agency (ESA) Ocean Colour Climate Change Initiative (OCCCI; Jackson et al., 2017), but revisited with coastal environments as a focus.

Under *TAPAS*, this fuzzy classification has been optimised to allow for hundreds of millions of remote sensing spectra to be considered as part of the training library, while attributing any single spectrum a membership to every class. This approach supports the spatial binning of algorithms, which in turn removes 'hard boundaries', which may occur in the case of switching algorithms, and also allows for optical complexity to be better represented. This approach can be applied to any optical sensor, but has been applied here to a catalogue of ESA Ocean and Land Colour Instrument (OLCI) and MEdium Resolution Imaging Spectrometer (MERIS) scenes that contain as diverse a set of coastal environments as possible. The method iteratively converged on twelve representative spectra, with each spectrum corresponding to an OWT (Fig. 2.1).

Remotely sensed reflectance can now be compared to *in situ* observation data of both reflectance and derived water column properties, on a type-by-type basis that will allow the mapping of suitable algorithms to each OWT. This provides the necessary flexibility in the system to produce satellite products in locations where *in situ* observations are lacking. However, it also exposes gaps in the *in situ* observation data sets where insufficient calibration and validation data are available to optimise and assess the accuracy of OWT-specific algorithm solutions.

This project has received funding from the EU H2020 research and innovation programme under Grant Agreement No 678396

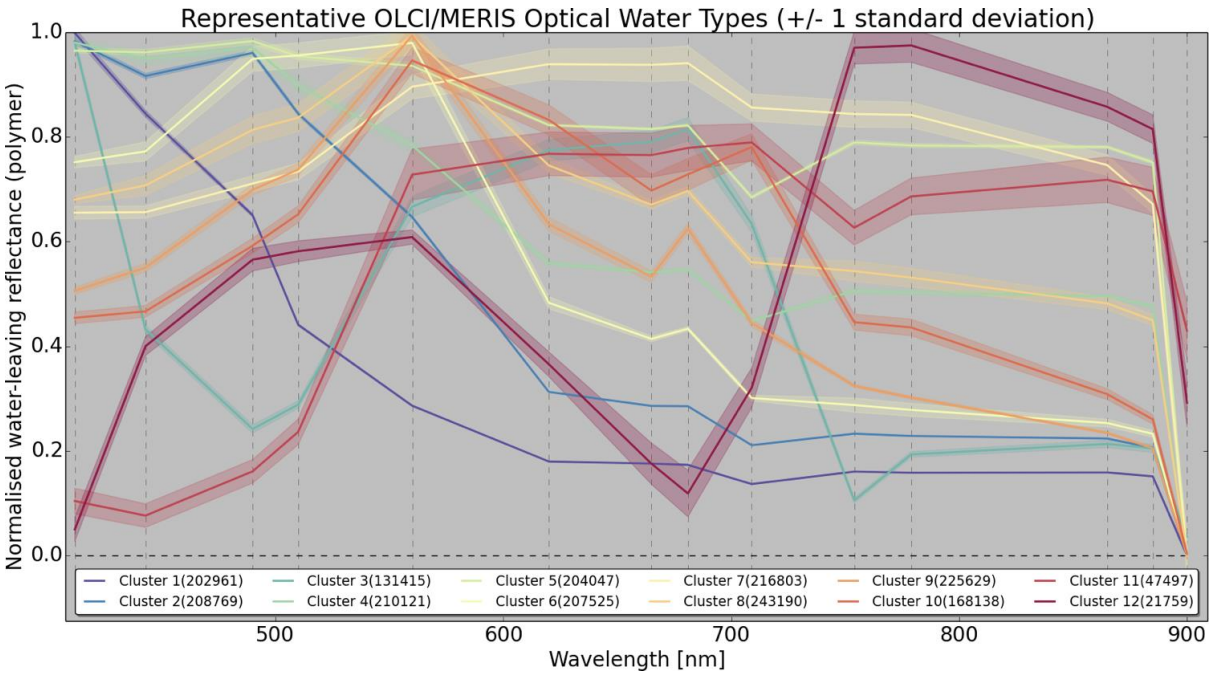

Figure 2.1. Representative spectra associated with the 12 optical water types identified by the coastally-focussed clustering algorithm. Each water type is associated with a set of optimised algorithms for chlorophyll-a and turbidity or total suspended matter concentration.

Although OWTs can be used to determine algorithm selection, they are also useful in their own right. Changes in OWT at a given location may be indicative of changes in the underlying environmental paradigm. Consequently, the OWTs have been mapped to the North East Atlantic and Mediterranean self-organising map zones (Figs. 2.2, 2.3). These maps are produced at 300 m resolution (the native resolution of OLCI), and will be subset to specific regions once the full processing (two years) is complete.

This project has received funding from the EU H2020 research and innovation programme under Grant Agreement No 678396

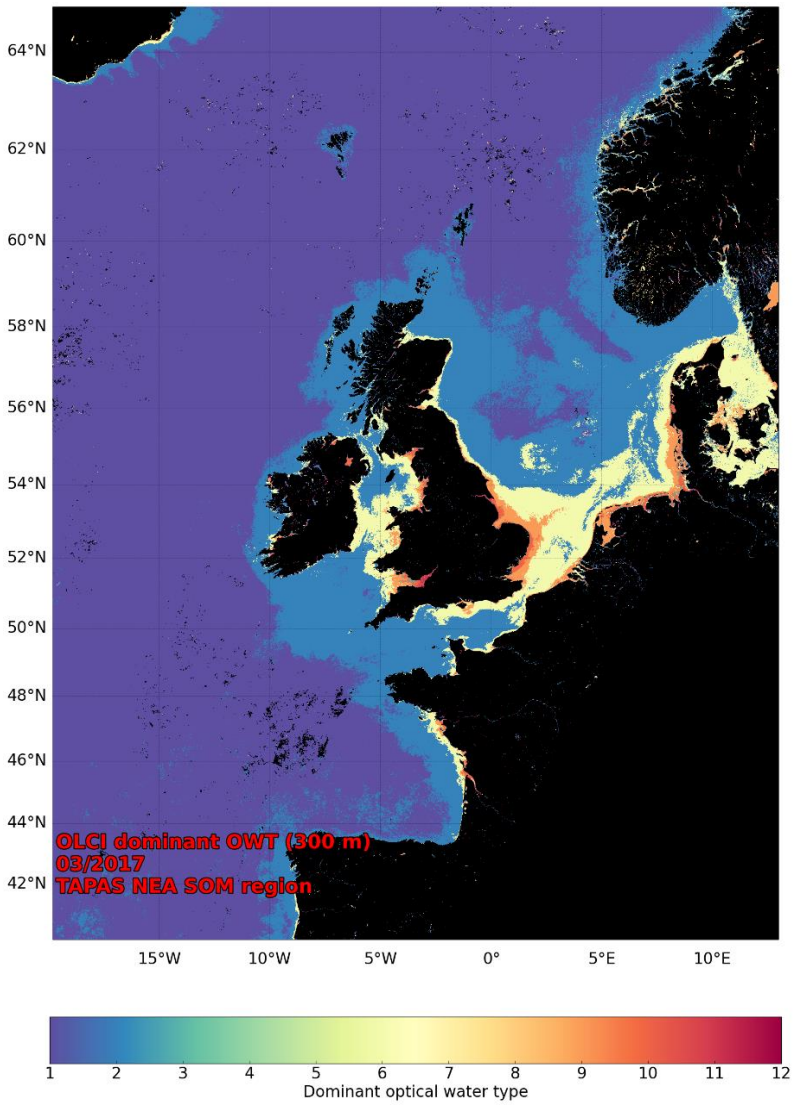

Figure 2.2. Spatial distribution of dominant optical water types across the North East Atlantic (NEA) self-organising map region for March 2017.

This project has received funding from the EU H2020 research and innovation programme under Grant Agreement No 678396

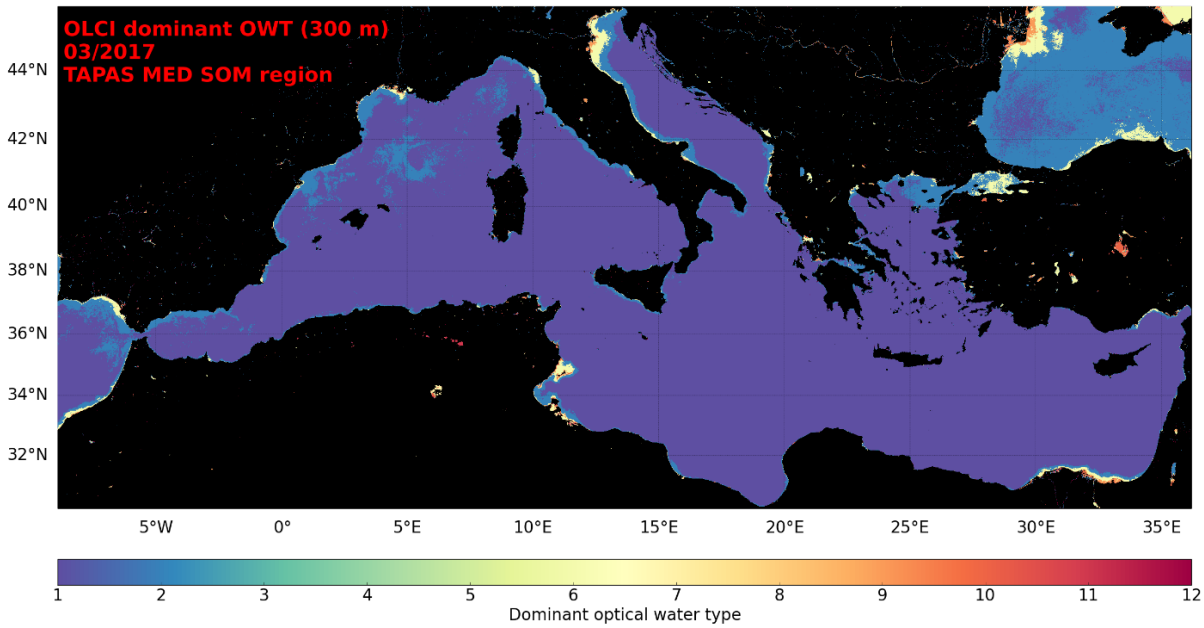

Figure 2.3. Spatial distribution of dominant optical water types across the Mediterranean (MED) self-organising map region for March 2017.

OWTs 1 (“open water”), 2 (“transitional water”), and the further coastal types 6, 9, and 10 are most frequently encountered, with the latter three capturing gradual changes in optical complexity around coastal regions. Turbidity and TSM algorithm sets have been validated for these OWTs, using data collated from the ESA OCCCI *in situ* data set, Centre for Environment, Fisheries and Aquaculture Science smart buoy network, Scottish Environment Protection Agency estuarine moorings and various cruise data. No turbidity and TSM algorithms have been assigned to the other OWTs due to a lack of validation data. The 1%, 5%, 95%, and 99% values for TSM and turbidity will also be provided for each pixel on an annual and month-by-month basis, providing information on the environmental envelopes associated with each region. CHL algorithm selection is currently in process. CHL products will be generated using the same approach as TSM.

2.3 Suspended particulate matter (SPM): extreme levels as indicator

Extreme levels of suspended particulate matter (SPM) have the potential to limit aquaculture due to its impact on food and light availability. We therefore mapped regions which regularly see SPM levels above a moderate threshold (60 mg/L) and two high thresholds (120 and 190 mg/L), based on existing analysis of the impacts of SPM on oysters (Gernez et al. 2014). SPM was calculated using OCCCI v4.1 satellite reflectance data and the SPM algorithm of Han et al. (2016), which was tuned to be able to detect high SPM levels. Daily reflectance data was downloaded for the period 1997-2019. We then converted this to SPM using the Han et al. (2016) algorithm, and calculated the maximum SPM in each year, and then identified regions where this maximum exceeded the three thresholds in the majority of years. These regions (figure) are largely restricted to coastal regions of high riverine input. Shellfish aquaculture

This project has received funding from the EU H2020 research and innovation programme under Grant Agreement No 678396

sites across most of the English, Dutch, Belgian and German coasts are likely to experience moderate SPM levels (> 60 mg/L). In contrast, the Mediterranean, and Spanish coasts largely see non-harmful levels of SPM. Most of the North French sees few regions of high SPM, however the Atlantic coast sees large regions with incidences of high SPM. Regions with high SPM levels are more restricted geographically. There is no detectable region where SPM regularly exceeds 190 mg/L.A small number of regions has SPM levels exceeding 120 mg/L, including the East Anglian Plume, parts of the central western French coast, and the northern Belgian coast.

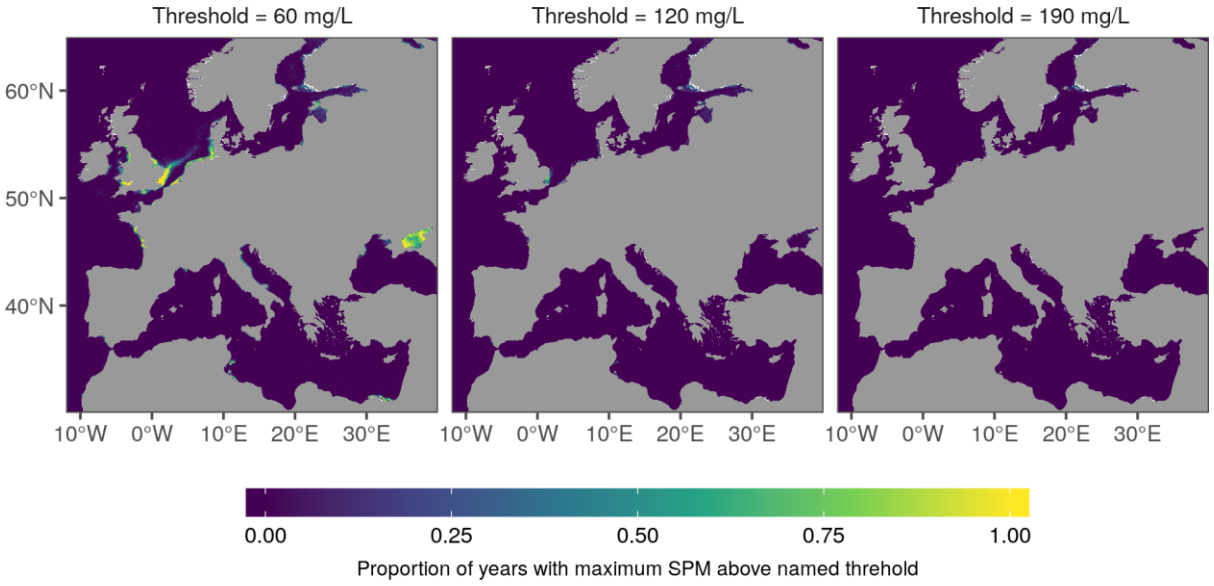

Figure 2.4. Proportion of years between 1997 and 2018 where SPM is above 60, 120, and 195 mg/L. SPM was calculated using daily OCCCI reflectance data and an algorithm for estimating SPM in highly turbid waters (Han et al. 2016).

2.4. Long-term risk of certain HAB species from satellite ocean colour indicators

There have been many previous applications of satellite ocean colour data for the aquaculture industry, mostly focussed on the near-real time early warning of harmful algal blooms (HABs) affecting aquaculture sites. As we continue to improve and validate HAB risk maps (Fig. 2.5; Kurekin et al., 2014), the estimation of the long-term probability of particular HAB types around the UK is increasingly feasible through analysing historical data.

This project has received funding from the EU H2020 research and innovation programme under Grant Agreement No 678396

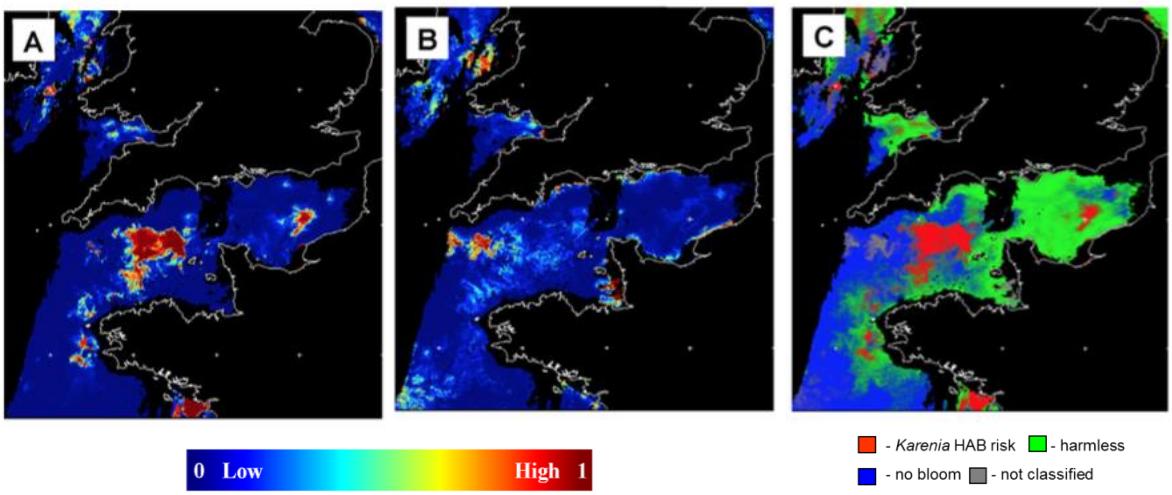

Figure 2.5. Examples of harmful algal bloom (HAB) discrimination using EO ocean colour data. a) Classification of spectra of each pixel in the image based on similarity to known *Karenia mikimotoi* harmful blooms. b) Accounting for unknown cases to prevent misclassification. c) Composite HAB risk over seven days of satellite data to minimise cloud gaps (Kurekin et al., 2014).

We have generated an initial seven-year analysis of the risk of *Karenia mikimotoi* occurrence in NW European waters, a species which can kill farmed salmon. Figure 1.6 depicts the total number of times events were classified as 'Harmful' in weekly EO risk maps from 2011 to 2017; note that this is not normalised to the varying quantity of valid ocean colour data due to cloud cover. Even the light purple regions have seen significant blooms of this HAB type; but if these only last a few weeks and do not appear every year in the same place, they do not aggregate a high probability over the seven-year integration. A similar analysis has been attempted for *Pseudo-nitzschia*, a potentially toxic species that can result in the closure of shellfish farms. This is undergoing further validation and improvements.

This project has received funding from the EU H2020 research and innovation programme under Grant Agreement No 678396

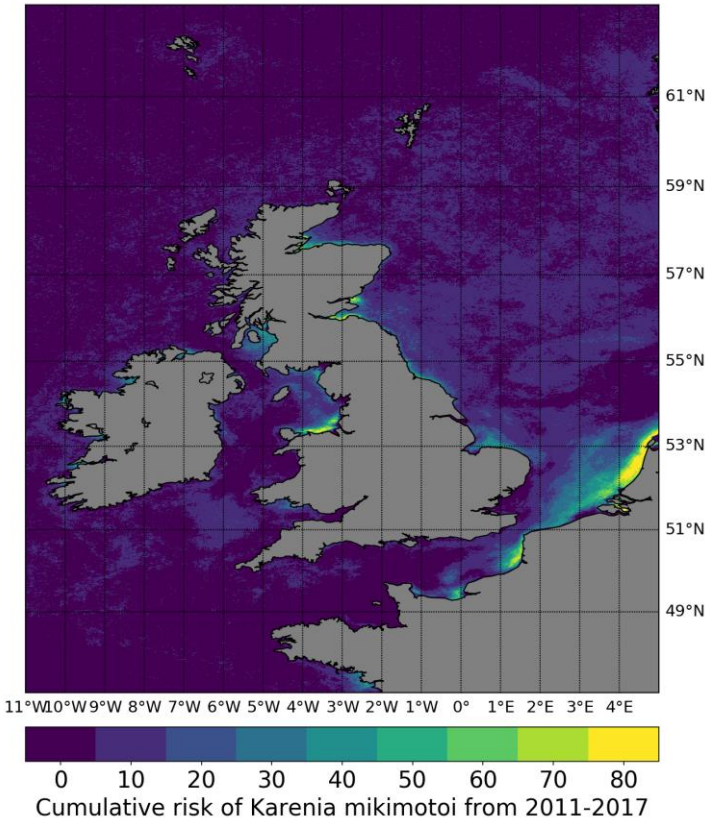

Figure 1.6. Number of harmful algal bloom events captured in weekly EO *Karenia mikimotoi* HAB risk maps.

Figure presents a time series of the same *Karenia mikimotoi* HAB risk dataset, for the entire UK continental shelf region shown in Fig. 2.6. It is also possible to generate this analysis for sub-areas to compare the seasonal and interannual variability of risks for different regions. These innovative satellite-based long-term HAB risk maps can support the aquaculture industry by enabling region-specific risk assessment. Patterns and trends will help to plan for new sites and to assess any potential change in risk at existing sites.

This project has received funding from the EU H2020 research and innovation programme under Grant Agreement No 678396

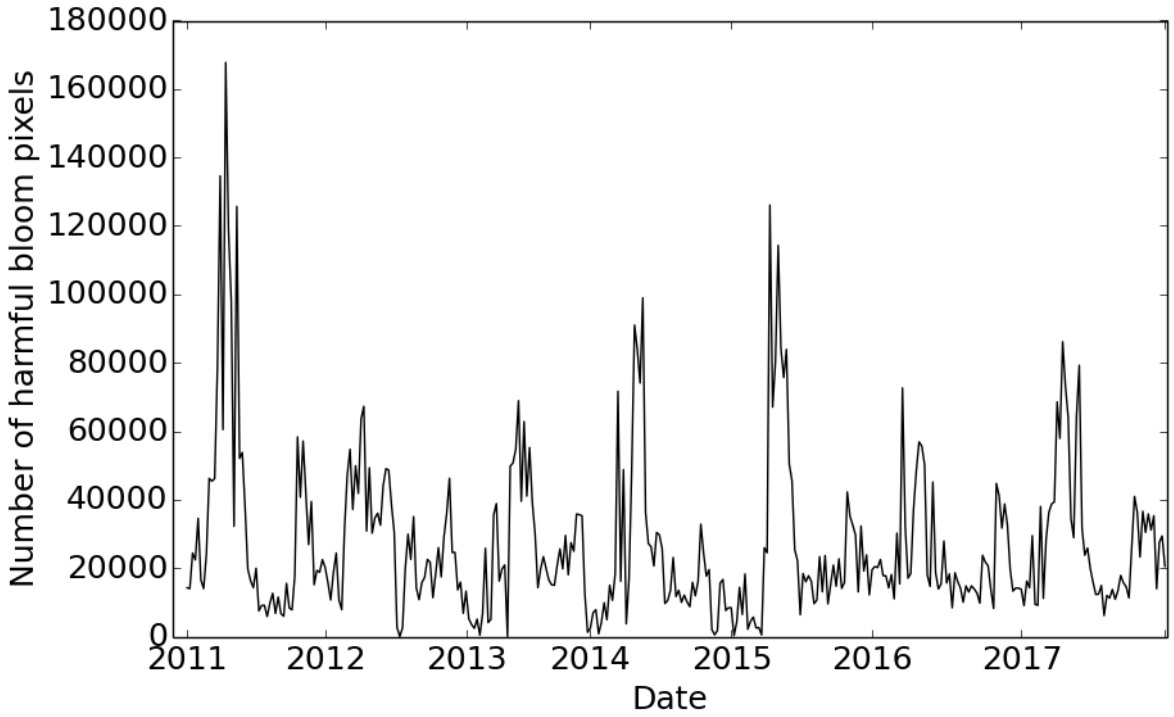

Figure 2.7. Number of weekly *Karenia mikimotoi* harmful algal bloom pixels in the EO ocean colour time series, for the entire UK continental shelf region shown above.

This project has received funding from the EU H2020 research and innovation programme under Grant Agreement No 678396

3. Assessing future suitability for shellfish aquaculture across Europe, based on projections from a POLCOMS-ERSEM model

3.1. Introduction

This section presents indicators of current and future suitability for aquaculture in European seas, derived from the output of an ecosystem model that covers both the Mediterranean Sea and the North west European shelf sea (Section 3.2). In particular, we present maps of indicators such as water temperature (influencing the physiology of commercial shellfish aquaculture species), phytoplankton and zooplankton biomass (influencing food availability for the upper marine trophic levels) and maps of degree days for Pacific oyster (*Crassostrea gigas*) expansion (Section 3.3).

3.2. The European marine ecosystem model

POLCOMS-ERSEM is a 3D hydrodynamic-biogeochemical ocean model suitable for modelling environmental conditions in coastal and shelf seas. POLCOMS (the Proudman Oceanographic Laboratory Coastal Ocean Modelling System, Holt and James 2001) provides the physical components: it models the motion of the water and the transfer of energy and momentum under the forcing provided by the surface conditions. ERSEM (the European Regional Seas Ecosystem Model, Butenschön et al., 2016) is the biogeochemical model: it includes key processes such as plankton photosynthesis, respiration and excretion, nutrient uptake and calcification. Carbon, nitrogen, phosphorus and silicon are each tracked separately and the biological components are represented by four phytoplankton functional types, three zooplankton and bacteria. There is also a benthic component modelling processes at the sea floor. The two models are coupled so that POLCOMS provides ERSEM with information about physical variables such as temperature and light levels and models the advection of nutrients and biological material. The model domain includes the North East Atlantic, the North Sea and the Mediterranean (Figure 3.2); the model resolution is 0.1° (approximately 11 km).

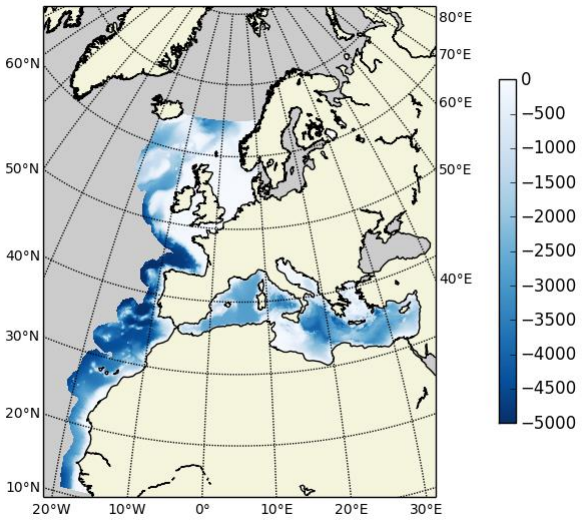

Figure 3.3 Model domain and bathymetry.

This modelling system was used to project environmental conditions for European seas over the 21st century under two scenarios of atmospheric greenhouse gas concentrations These scenarios used two of the standard Representative Concentration Pathways (RCPs) used by the Intergovernmental Panel on Climate Change (van Vuuren et al., 2011): RCP 4.5 is a moderate scenario, with concentrations rising until mid-century then stabilising, and RCP 8.5

This project has received funding from the EU H2020 research and innovation programme under Grant Agreement No 678396

is a more extreme scenario, with concentrations higher and rising all century. The model was driven using global climate model MPI-ESM-LR[1]. MPI-ESM-LR was selected as best representing the range of conditions projected by those models for which regionally-downscaled atmospheric model outputs and a consistent set of river run-off values were available. At the atmosphere-ocean interface meteorological conditions were taken from the downscaled regional climate model MPI-ESM-LR-RCA4[2] (resolution 0.11°; downloaded from EURO-CORDEX, www.euro-cordex.net). Global model outputs were used at the open ocean boundary, for both physical and biogeochemical conditions. Daily projected values for river discharge and N and P loadings were taken from the hydrological model E-HYPE[3] (Donnelly et al. 2016), using the same global climate model and assuming current patterns of land use and other factors affecting river nutrients. Projections of change at the Baltic boundary were not available, so climatological water and nutrient flows were used, and these were kept constant through the modelled period. This means that modelled conditions in the Norwegian Trench may not fully reflect the effect of climate change. In addition, nitrate levels in the Norwegian Trench are overestimated compared to observed values: projections for the Norwegian Trench should be treated as relatively unreliable.

Outputs include key physical and biogeochemical variables for the pelagic and benthic systems, at daily and monthly frequency; also, sea surface elevation at hourly frequency.

The model outputs for sea surface temperature and chlorophyll concentration have been compared to satellite values for 1998-2015. Satellite chlorophyll data were sourced from the ESA Climate Change Initiative Ocean Colour project (http://www.esa-oceancolour-cci.org/, v3.1). Sea surface temperature is from the OSTIA dataset, downloaded from CMEMS (http://marine.copernicus.eu/, products SST_GLO_SST_L4_NRT_OBSERVATIONS_010_001 and SST_GLO_SST_L4_REP_OBSERVATIONS_010_011).

There is a good spatial and temporal match between modelled and satellite-derived sea surface temperature (Table 3.1 and Figure 3.2). Model-satellite correlation is high in all regions; correlations are weaker for the Atlantic regions than for the North Sea and Mediterranean. The model also broadly reproduces the temporal and spatial patterns of chlorophyll concentration across the region, but model estimates tend to be higher than satellite estimates, especially in regions of high chlorophyll. Model outputs are lower than satellite estimates in northern Europe during the winter, though it should be noted that satellite estimates can be inaccurate in these conditions because of high cloud cover and the confounding effect of CDOM and suspended particulate matter. The model-satellite correlation is weakest in shallow coastal areas, however satellite chlorophyll estimates are less reliable in these areas than for open seas.

[1] Max-Planck-Institute Earth System Model, Low Resolution; http://www.mpimet.mpg.de/en/science/models/mpi-esm.html
[2] Max-Planck-Institute Earth System Model, Low Resolution driving the Rossby Centre Regional Atmospheric model, version 4
[3] HYdrological Predictions for the Environment, European domain

This project has received funding from the EU H2020 research and innovation programme under Grant Agreement No 678396

Table 3.1 Model-satellite comparison for sea surface temperature and surface chlorophyll-a, using monthly data for 1998 to 2015, for the whole model domain and sub-regions. The Atlantic (North) region is from 46°N to 65°N, Atlantic South from 25°N to 46°N. Bias = model mean – satellite mean; RMSD = root mean square difference between model and satellite; Spearman-r = Spearman rank correlation coefficient.

	Sea surface temperature (°C)			Surface chlorophyll-a (mg m^{-3})		
Region	**Bias**	**RMSD**	**Spearman-r**	**Bias**	**RMSD**	**Spearman-r**
whole	0.07	1.26	0.98	0.67	1.61	0.60
Mediterranean	-0.19	1.14	0.97	0.22	0.64	0.48
North Sea	0.55	1.24	0.96	1.12	2.50	0.45
Atlantic (North)	0.37	1.28	0.90	0.82	1.74	0.58
Atlantic (South)	-0.46	1.06	0.94	0.92	1.56	0.57

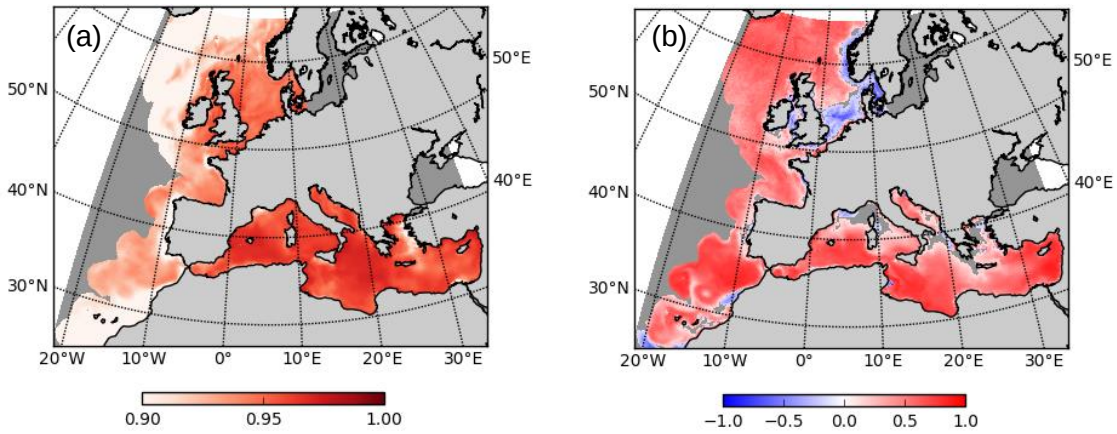

Figure 3.4 Spearman correlation between monthly mean and satellite values of (a) sea surface temperature and (b) surface chlorophyll concentration, 1998-2015.

3.3. Summary of European aquaculture drivers and indicators under changing climate scenarios

Projections of long-term changes in key aquaculture indicators were derived from POLCOMS-ERSEM model output. These indicators are summarized in Table 3.2. Each indicator was derived for a baseline historical period (1985-2005), a mid-century (2040-2059) and a late-century period (2080-2099) for both RCP 4.5 and 8.5.

Indicators were chosen on the basis of their relevance to multiple species and taking account of the list of regional sustainability indicators presented in Milestone M6.3 of *TAPAS*. Changes in nutrient availability, as indicated by variables such chlorophyll, phytoplankton, zooplankton and nitrogen, will influence future productivity of aquaculture. Similarly, physical variables such as temperature, salinity and current velocities will significantly impact the biological growth

This project has received funding from the EU H2020 research and innovation programme under Grant Agreement No 678396

potential of aquaculture and will influence the physical challenges of aquaculture. Finally, measures such as degree days are key indicators of ecological sustainability and the potential risk for aquaculture species to become invasive (Herbert et al. 2016).

Table 3.2 Summary of indicators calculated for climate change scenarios. Climatological indicators have been calculated for historical (1986-2005), mid-century (2040-2059) and late-century time periods (2080-2099) for the emissions scenarios RCP 4.5 and 8.5.

Indicator	Time scale	Indicator	Time scale
Chlorophyll-a	Monthly mean	Salinity	Monthly mean
Phytoplankton carbon	Monthly mean	Mixed layer depth	Monthly mean
Zooplankton carbon	Monthly mean	Ratio of dinoflagellates to diatoms	Monthly mean
Surface current velocities	Monthly mean	Total microplankton and nanoplankton carbon	Monthly mean
Particulate organic carbon	Monthly mean	Ratio of silicate to nitrogen	Monthly minimum and maximum
Dissolved oxygen at the surface	Monthly minimum	Ratio of silicate to phosphate	Monthly minimum and maximum
Sea surface temperature	Monthly mean	Ratio of phosphate to nitrogen	Monthly minimum and maximum
Seabed current velocities	Monthly mean	Nitrogen	Monthly mean
Silicate	Monthly mean	Phosphate	Monthly mean
Temperature above 20 °C	Mean proportion of days with temperature above 20 °C	Larval survival threshold	Proportion of years where temperature is above 22 °C for 15 consecutive days
Recruitment potential	Mean degree days before October, using biological zero for 10.55 °C.		

This project has received funding from the EU H2020 research and innovation programme under Grant Agreement No 678396

Figure 3.3 shows changes in sea surface temperature across the region during the 20th century under RCP 4.5 and 8.5. Temperature increases are universal across both scenarios, with the exception of regions at the model boundary, which are likely an artefact of boundary condition issues. Temperature increases are higher under RCP 8.5 at the end of the century, with increases of 3-4°C across much of the Mediterranean and 2-3 °C in much of the North Sea.

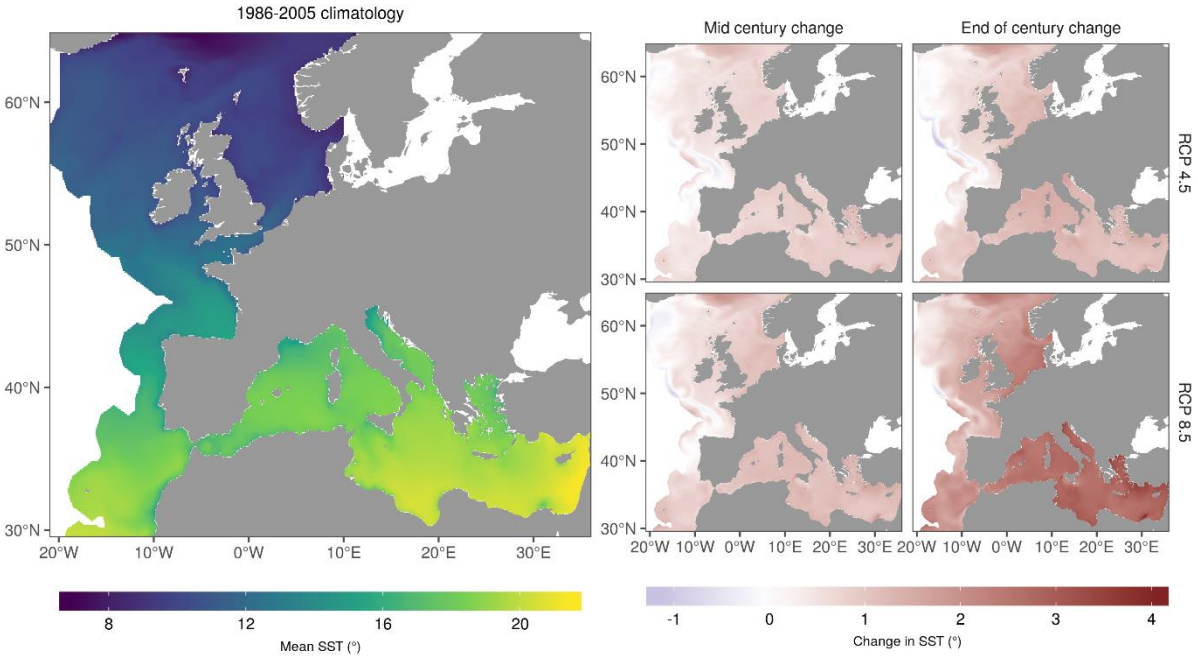

Figure 3.3. Left: Mean annual sea surface temperature for 1986-2005. Right changes in mean annual SST under the emissions scenarios RCP 4.5 and 8.5 by mid-century (2040-2059) and late-century (2080-2099).

Changes in phytoplankton and zooplankton carbon are shown in figures 3.4 and 3.5. Under both emissions scenarios there is a clear reduction in plankton carbon available in the North Sea, British Isles, and the French and northern Spanish coasts. This has the potential to negatively influence shellfish aquaculture production in these regions. There is an increase in plankton production in the Norwegian Trench, however this is likely a result of the boundary conditions issue discussed in section 3.2. In contrast, there is an increase in plankton carbon available across the Mediterranean Sea, implying that increased food availability could partly offset the negative impacts of temperature increase in this region.

This project has received funding from the EU H2020 research and innovation programme under Grant Agreement No 678396

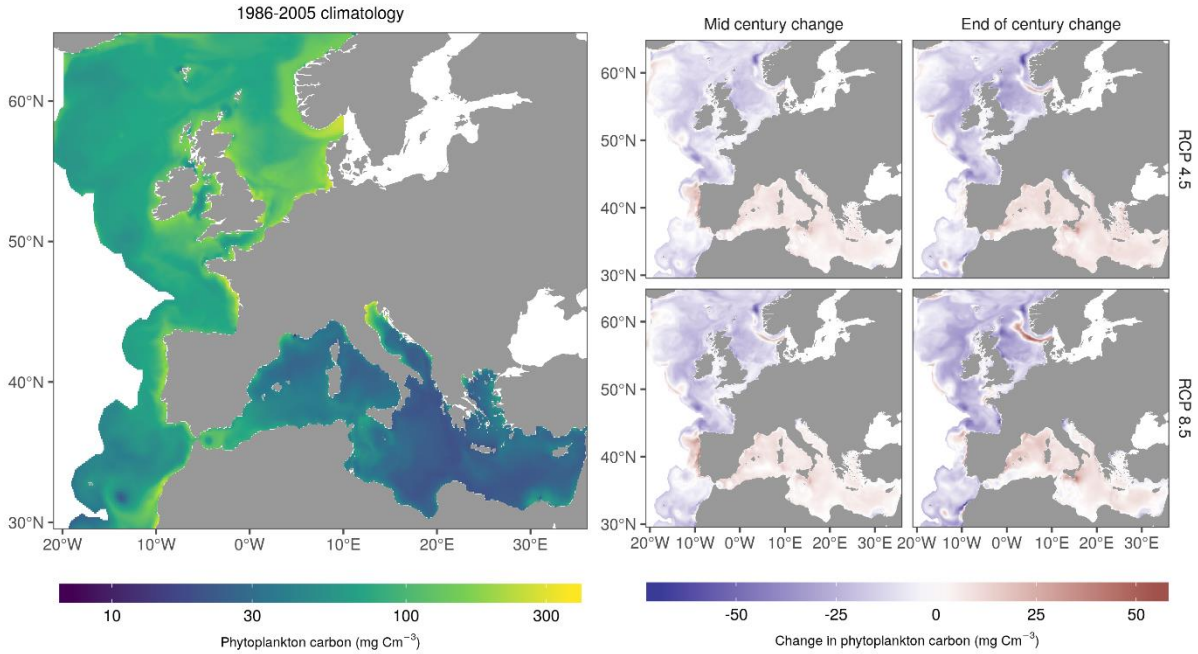

Figure 3.4. Left: historical baseline annual climatology of phytoplankton carbon. Right: absolute changes in mean annual phytoplankton carbon under the emissions scenarios RCP 4.5 and 8.5 by mid-century (2040-2059) and late-century (2080-2099).

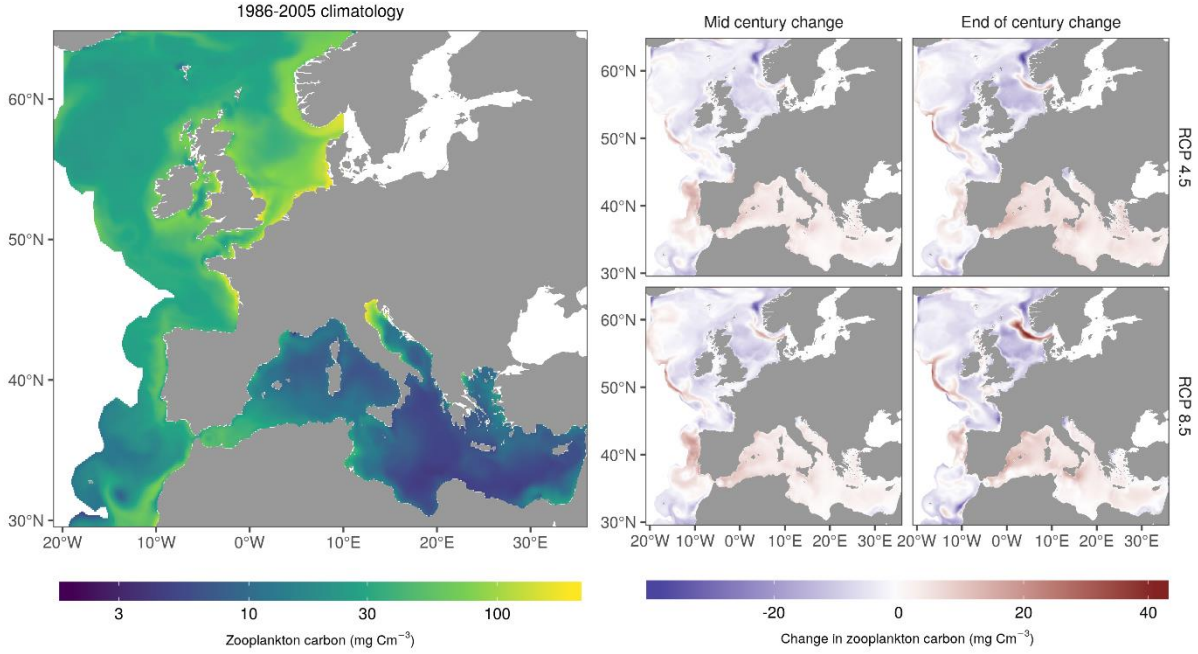

Figure 3.5. Left: historical baseline annual climatology of zooplankton carbon. Right: absolute changes in mean annual zooplankton carbon under the emissions scenarios RCP 4.5 and 8.5 by mid-century (2040-2059) and late-century (2080-2099).

A key indicator for whether a species can potentially become invasive is whether it can complete its life cycle. For Pacific oysters, this indicator can be split into two key sub-indicators: whether environmental conditions are sufficient for adults to spawn and 2) whether

This project has received funding from the EU H2020 research and innovation programme under Grant Agreement No 678396

post-spawning conditions are sufficient for larvae to metamorphose (Herbert et al. 2016, Thomas et al. 2016). Analysis of existing empirical data has shown that 600 degree days, using a biological zero of 10.55°C, is the approximate threshold for conditioning and spawning, while 825 degree days has been established as the requirement for larval metamorphosis (Syvret et al. 2008). In addition, there is an approximate threshold of 18°C for the triggering of spawning (Thomas et al. 2016), however there are suggestions from field studies that this threshold is too high (Shelmerdine et al. 2017). We therefore took an approach that took a simplified degree day method to mapping regions where oysters can spawn and metamorphose. This approach ignores changes in pH, food and fishing pressures which may have important impacts in regions (Lemasson et al. 2018, Pernet et al. 2016).

We mapped the regions where in the present, mid-century and end-of-century the 600 and 825 degree day threshold would be exceeded in the majority of years. The methodology for this was as follows. First, we calculated the degree days for each day. For each year we then calculated the running cumulative sum of degree days. We then identified the first day of the year when there were a total of 600 cumulative degree days and that temperature exceeded 18°C. This was classified as the earliest potential spawning date. Regions that met these criteria were classified as having spawning potential. In these regions we then calculated the number of degree days that occurred after the earliest potential spawning date. If this exceeded 225 degree days we classified a region as having metamorphosis potential.

Figure 3.6 shows that there will be a large northward shift in regions which exceed these thresholds. In the historical baseline period Pacific oysters are incapable of reaching the metamorphosis stage on the entire English Coast, with the exception of the East Anglian Plume reach, and the species is furthermore incapable of reaching the spawning stage on the Irish or Scottish coasts. Under the high emissions RCP 8.5 scenario Pacific oysters are capable of reaching metamorphosis across almost the entire English coast and southern and central North Sea. In the lower emissions scenario RCP 4.5 approximately half of the English coast has conditions which allow oysters to metamorphose. A key difference between the scenarios RCP 4.5 and 8.5 is that oysters are incapable of spawning on the Irish coastline in RCP 4.5, but are capable of spawning across over a third of the Irish coast in RCP 8.5. It is therefore clear that there will be both significant potential for new Pacific oyster aquaculture in northern regions (see also Thomas et al., 2016), but also potential ecological consequences of an invasion of this species (Reise et al. 2017). These maps have the potential to identify areas which are currently unfarmed, but with aquaculture potential, and also to show those that are likely to become potential aquaculture sites in future.

This project has received funding from the EU
H2020 research and innovation programme
under Grant Agreement No 678396

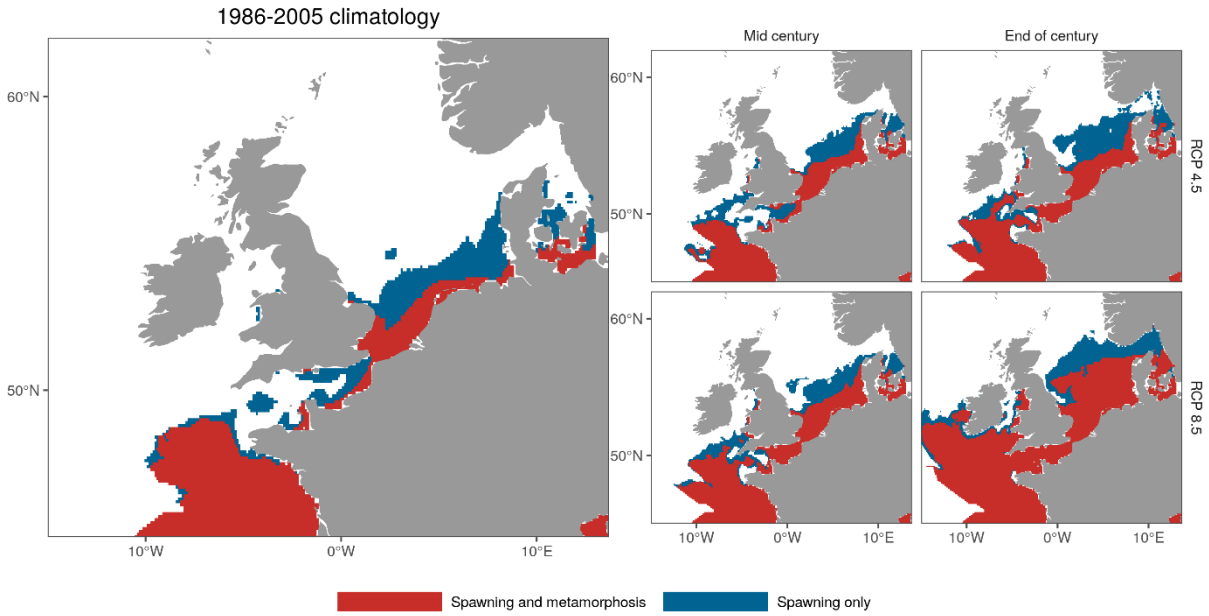

Figure 3.6. Regions of recruitment potential for Pacific oyster. Blue regions are those wherein the majority of years temperatures meet the requirement for conditioning and spawning, but not for metamorphosis (600 degree days attained by September and that SST exceeds the 18°C threshold required for spawning). Red regions are those where temperatures are also sufficient for larvae to metamorphose (600 degree days available for conditioning and spawning and a further 225 degree days after a time when temperature exceed 18°C). Degree days are calculated using a biological zero of 10.55°C. 825 degree days is required to achieve larval metamorphosis.

This project has received funding from the EU H2020 research and innovation programme under Grant Agreement No 678396

4. POLCOMS-ERSEM-driven Dynamic Energy Budget modelling of Pacific oyster growth potential: aquaculture indicators for the offshore environment

4.1. Background

The increase in and expansion of aquaculture and other human activities in the nearshore coastal environment has resulted in this limited space being under increased competition between potential uses. At the same time, projected population growth and the increasing role of aquaculture in overall seafood provision, are expected to further increase the demand for marine aquaculture (FAO, 2018). Extending aquaculture production further offshore than has traditionally been practiced has been identified as one potential solution to this issue (Gentry et al., 2017). Moving offshore, even if coupled with other offshore industries, such as wind energy farms (Buck and Langan, 2017) to leverage infrastructure investments, requires substantial initial and ongoing investments. Site selection to ensure the feasibility and sustainability of aquaculture investments and activities is therefore crucial (Gentry et al., 2017, Brigolin et al., 2017, Barillé et al., submitted). Furthermore, aquaculture is relatively novel in the offshore environment, compared to the nearshore coastal environment where it has conventionally taken place over the past decades and even centuries. More information about whether and where cultivated organisms can be expected to thrive in these new environments is needed. In the context of site selection, such information needs to be spatially-explicit.

A further consideration in assessing the cost-benefit and feasibility of investing in offshore aquaculture are whether and where these would be expected to be sustainable, particularly in light of ongoing and uncertain climate change. Although what climate conditions will be over the next century remains highly uncertain, dependent upon a range of possible emissions scenarios now and into the future (Moss et al., 2010; Gattuso et al., 2015), biogeochemical and hydrodynamic models improve our understanding of how ocean conditions can be expected to change as a result (IPCC, 2019). Such model outputs, from POLCOMS-ERSEM (see Section 3), are used here to drive Dynamic Energy Budget (DEB) modelling of Pacific oyster, *Crassostrea gigas*, in order to assess its offshore growth potential over a broad geographic scale from north-western Africa to northern Europe. In addition to providing maps and insight into baselines for Pacific oyster growth potential based on an early-century reference period, POLCOMS-ERSEM data were generated for two late-century climate scenarios and used in DEB modelling to forecast future sector potential and assess the variability in oyster growth potential in light of climate change uncertainty. Multi-temporal growth maps for all scenarios are transformed into industry-relevant indicators of the current growth potential and future sustainability in light of climate change. Such information supports decision-making and management at the regional scale, providing information on which areas should be prioritized for further consideration for finer-scale site selection.

4.2. Description of the modelling approach

Dynamic energy budget (DEB) theory is a generic way to mechanistically model energy flow through an individual organism (Kooijman, 2010), from food ingestion through maintenance, growth, and reproduction. It has been adapted and applied to many species, and an adaptation

This project has received funding from the EU H2020 research and innovation programme under Grant Agreement No 678396

put forth by Pouvreau et al. (2006) for the Pacific oyster, *Crassostrea gigas*, and further parameterized by Bernard et al. (2011) and Thomas et al. (2016), is used here (Fig. 4.1). In the Pacific oyster DEB applied here, ingestion and maintenance are affected by water temperature (Temp. in Fig. 4.1), and ingestion is further affected by food (phytoplankton) abundance (Food in Fig. 4.1), modulated by a calibrated model parameter, the half-saturation coefficient (X_k). Given the range of turbidity variability in the offshore ocean, the impact of too high turbidity on the half-saturation coefficient was not taken into account. All model equations and other parameter values can be found in Thomas et al. (2016 S1).

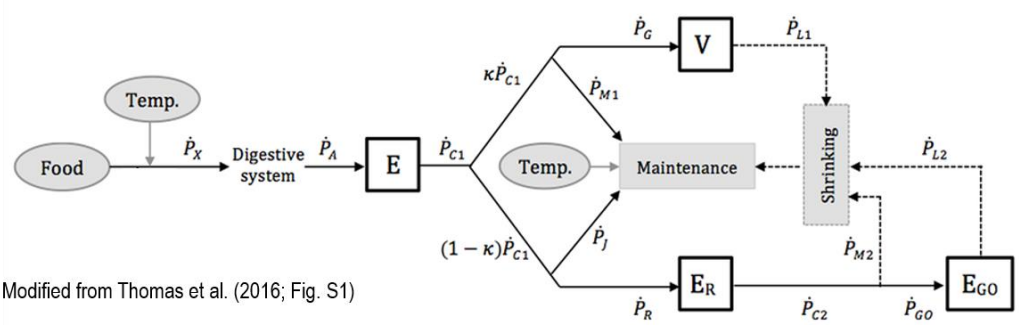

Figure 4.1. Schematic of dynamic energy budget (DEB) model used to model Pacific oyster growth and reproduction.

Input data for the current Pacific oyster DEB modelling was chlorophyll-a (chl-a) concentration as a proxy for food abundance, and water temperature output at the daily time step and 0.1° spatial resolution from the surface layer (~ 5 m depth) of the three-dimensional coupled hydrodynamic-biogeochemical ocean model, POLCOMS-ERSEM, described in greater detail in Section 3 of this report. Chl-a was provided for four particle size ranges. The smallest size class (picoplankton; < 2 µm) was excluded, as this is not retained by the gills of *C. gigas*; concentrations of the remaining three classes were summed to produce the chl-a time series maps used. In addition to the daily chl-a and water temperature maps, daily salinity (psu) and current speed (m s^{-1}) maps were also generated. A single bathymetry map of the model domain for the three scenarios was also used. These were used to constrain threshold-based suitable areas within which to map DEB-modelled growth potential, to then generate industry indicators.

In situ measurements to calibrate the ingestion half-saturation coefficient (X_k) of the DEB model, and to validate model outputs are rare, given the novel and often experimental or confidential nature of offshore oyster cultivation. However, data from two regions within the POLCOMS-ERSEM domain for which DEB modelling of Pacific oyster was carried out were identified (Fig. 4.2): the German Bight of the North Sea (published in Pogoda et al., 2010; Fig. 4.2b) and the centre of Bourgneuf Bay on the French Atlantic coast (from experimental work carried out there by an association supporting shellfish growers and fishers in the region (*Syndicat Mixte pour le Développement de l'Aquaculture et de la Pêche en Pays de la Loire (SMIDAP)*; Fig. 4.2c). Data from one of the two years for which measurements are available from Bourgneuf Bay were used to calibrate X_k (Fig. 4.3a) through optimization regression, and the remaining French and German data were used to validate model outputs (Fig. 4.3b). For calibration and validation, the model was run for the specific date range for which measurements were available and using initial oyster sizes reported. Modelled values coinciding with the locations and dates of *in situ* measurements were extracted.

This project has received funding from the EU H2020 research and innovation programme under Grant Agreement No 678396

For measured data reported in Pogoda et al. (2010), only the month of measurement was reported, so this was taken to be the middle (15th) of each measurement month to approximate, and represents a source of uncertainty. Furthermore, although *in situ* measurements are from the location of a single cage, the spatial resolution (i.e., pixel size) of the POLCOMS-ERSEM data is 0.1°, which corresponds to approximately 11km. Although these spatial and temporal sources of uncertainty are expected to negatively affect validation results, modelled total weights are found to correspond well to those measured *in situ*, using a single calibrated X_k value (13.4).

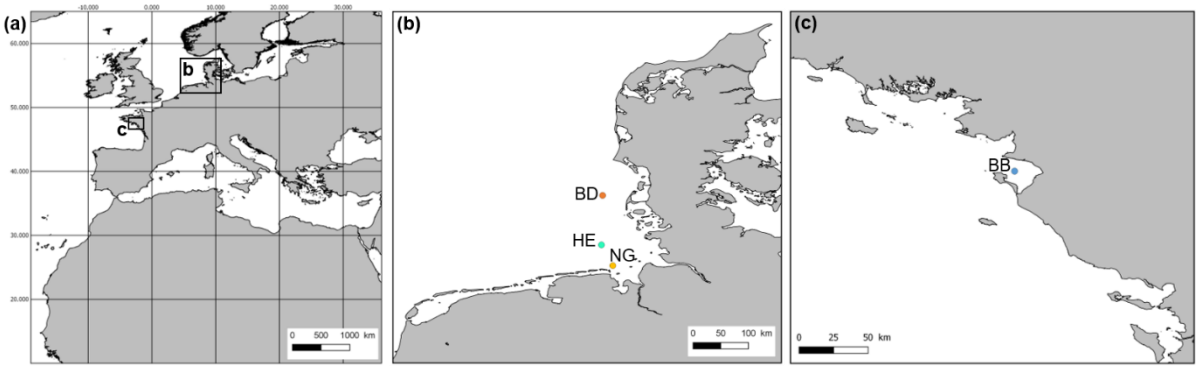

Figure 4.2. (a) Extent of ERSEM-POLCOMS domain, used as input for Pacific oyster DEB modelling; regions with *in situ* data used for model calibration and validation are highlighted. (b) Validation sites in the German Bight of the North Sea; Butendiek (BD), Helgoland (HE), and Nordergründe (NG), from Pogoda et al. (2011). (c) Calibration (2010) and validation (2008) data from Bourgneuf Bay, France.

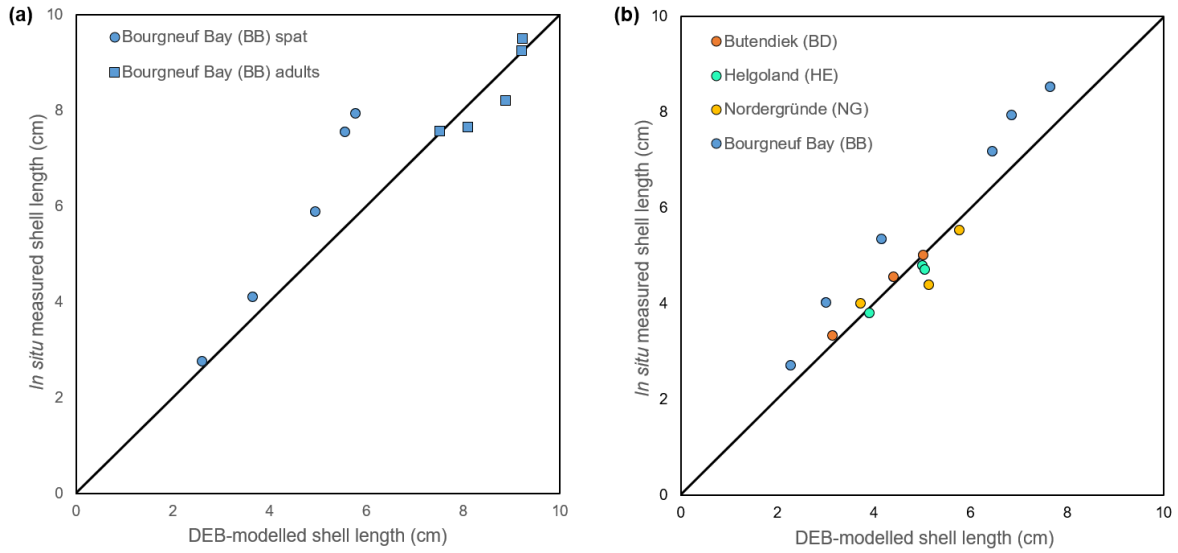

Figure 4.3. (a) Half-saturation ingestion coefficient, X_k, calibration using *in situ* data from Bourgneuf Bay (BB), France (2010. (b) Validation of Pacific oyster dynamic energy budget modelling with calibrated X_k (= 13.4) using separate *in situ* data from Bourgneuf Bay (BB), France (2008) and Germany (Butendiek (BD), Helgoland (HE), 2004; Nordergründe (NG), 2007 (Pogoda et al., 2010)).

This project has received funding from the EU H2020 research and innovation programme under Grant Agreement No 678396

The calibrated X_k value was then used in model initialization along with set oyster sizes and date ranges for each production stage (spat pre-grow, adult grow-out, and fattening or finishing (Table 4.1) to run the DEB model for an early century reference and two climate change scenarios (Table 4.2). To assess potential climate change impacts on oyster growth and aquaculture potential, two of the four representative concentration pathways (RCPs) were selected, and POLCOMS-ERSEM data for the period 2090-2099 were generated for each: RCPs 4.5 and 8.5 (Table 4.2). Under RCPs 4.5 and 8.5, radiative forcing associated with greenhouse gas emissions stabilizes at 4.5 W m^{-2} and exceeds 8.5 W m^{-2} by 2100 respectively (Moss et al., 2010). The latter is therefore to be a more extreme climate scenario. Both are compared here with modelled POLCOMS-ERSEM data which assimilates ocean colour data observations for the period 2000-2004 (Table 4.2). This early century reanalysis reference data are expected to be more realistic than model projections alone, as modelled data are corrected toward observed values, and errors in both are accounted for (Ciavatta et al., 2016).

Table 4.1. Model initialization of oyster size and modelled duration for the three production stages considered.

Production stage	Initial oyster size	Start date	End date
Spat pre-grow	0.5 g total weight 1.9 cm shell length 0.05 g dry flesh mass	April 1	December 1
Adult grow-out	14 g total weight 5.7 cm shell length 0.3 g dry flesh mass	April 1	December 1
Finishing/fattening	76 g total weight 10 cm shell length 0.9 g dry flesh mass	September 1	December 1

This project has received funding from the EU H2020 research and innovation programme under Grant Agreement No 678396

Table 4.2. Summary of the three scenarios for which ERSEM-POLCOMS data were generated and used to run DEB modelling.

Scenario	Years	Modelled data
Early century reference	2000-2004	Historic data assimilated
Late century climate change RCP 4.5	2090-2099	RCP 4.5 projection
Late century climate change RCP 8.5	2090-2099	RCP 8.5 projection

Prior to mapping the oyster growth potential indicators, a suite of binary biological requirement thresholds based on reported Pacific oyster tolerance ranges was applied across the model domain for each of the three scenarios to constrain the suitable area for Pacific oyster cultivation. This made use of additional POLCOMS-ERSEM daily map data on salinity, bathymetry, and current, in addition to SST and chl-a, also used in DEB modelling. The tolerated ranges of Pacific oyster for each of these were obtained from the literature, and are summarized in Table 4.3. A given pixel was considered to be suitable if, over the full average year for the given scenario, it remained within the tolerance range within a 95% confidence interval, as per Kapetsky et al. (2013). The bathymetric range of <= 200m, related to technical industry limitations, from Gentry et al. (2017) was also applied. Neither SST nor salinity were found to limit the suitable range here. The suitable spatial extents for each of the other variables, and the combined resulting final suitable area are visualized in Fig. 4.4.

Table 4.3. Documented Pacific oyster tolerance ranges for several variables used to constrain the suitable cultivation area, within which relative growth potential was assessed.

Variable	Documented tolerance range	Reference
Salinity	15-45 psu	Nell & Holliday (1988)
Current	Current 0.1-1 m s^{-1}	Kapetsky et al. (2013)
SST	3-35°C	Bayne (2017)
Chl-a	> 1 mg m^{-3}; > 4 µm particles	Barillé et al. (1993)

This project has received funding from the EU H2020 research and innovation programme under Grant Agreement No 678396

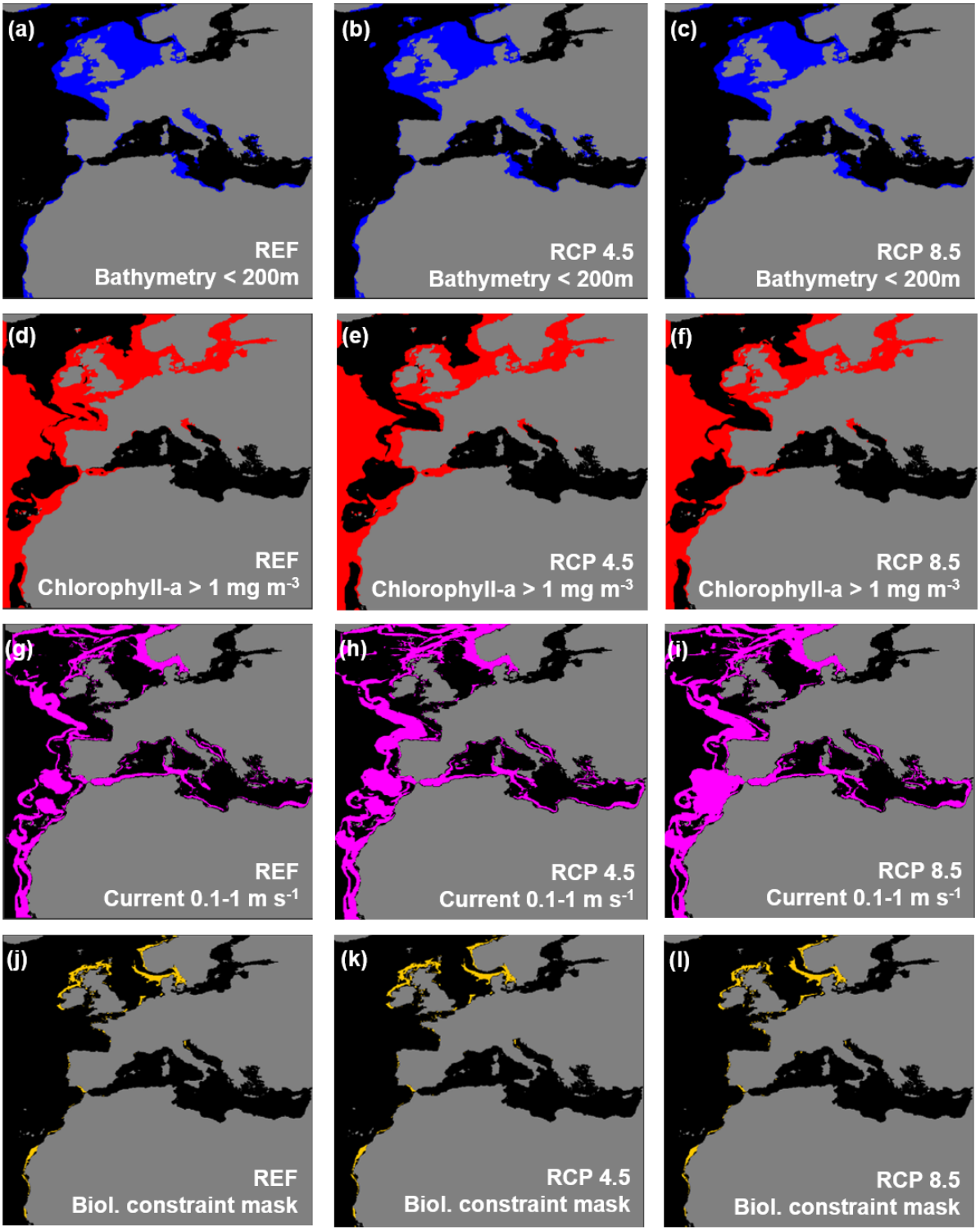

Figure 4.4. Biologically feasible areas for Pacific oyster growth for several constraining parameters, (a-c) bathymetry, (d-f) Chl-a, and (g-i) current speed, and their combined masks, used here (j-l); other potentially-limiting factors (SST and salinity) were not found to be constrain any area in the input dataset used here. Bathymetry is considered a constraint from a technical perspective.

This project has received funding from the EU H2020 research and innovation programme under Grant Agreement No 678396

4.3. Model outputs & oyster aquaculture indicators

Outputs from DEB modelling using the POLCOMS-ERSEM input data are maps of Pacific oyster shell length (L; cm), dry flesh mass (DFM; g), and total weight (TW; g) (e.g., Fig. 4.5), calculated allometrically from L, at the same temporal (i.e., daily) and spatial (i.e., 0.1°) scales as the input data, and for the spatial coverage (western Europe and north-western Africa) and date range defined in the model initialization; in this case April 1 to December 1 for both the spat pre-growing and adult grow-out phases, and September 1 to December 1 for the final fattening or finishing period (Table 4.1). The model was run, and these outputs were generated for each year of the three scenarios described above (early century reference, late century RCP 4.5, and late century RCP 8.5; Table 4.2). A mean year for each of these was then used to generate indicators and for comparison.

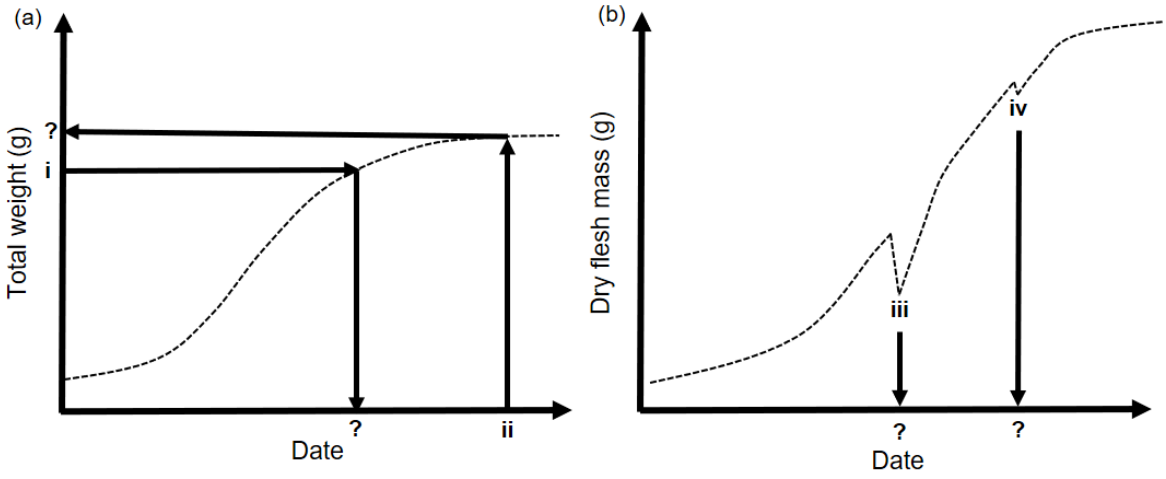

Figure 4.5. Examples of modelled Pacific oyster (a) total weight, calculated allometrically from shell length and (b) dry flesh mass generated at the daily time step and for each 0.1° pixel of the ERSEM-POLCOMS input data. The date a target weight is achieved (i), or, inversely, the weight achieved by a certain date (ii), can then be mapped. Abrupt, negative spikes in (b) correspond to spawning events (iii, iv), the timing or number of which can also be mapped as indicators (from Palmer et al., submitted).

Mapped growth time series were then transformed into a suite of industry-relevant aquaculture indicators associated with each of the production cycle stages (i.e., spat pre-growing, adult grow-out, finishing/fattening), and mapped for each of the reference and two climate change scenarios. An example of each, for the early century reference period and for the full model domain, is found in Fig. 4.6. Spat and adult indicators are related to the time it takes to reach a target total weight of interest, the total weight achieved by a date of interest, and the timing and number of spawning events (Figure 4.5; Table 4.4). In terms of finishing, Quality Index (QI) is the ratio of flesh to total weight. It is used to assess essentially the fullness of the oyster, and is related to French market classes (*Normales* (QI < 6.5%), *Fines* (6.5%< QI < 10.5%), and *Spéciales* (QI > 10.5%); Gosling, 2003; AFNOR, 1985), which are associated with increasingly higher prices. To estimate QI, since flesh weight is not modelled, it is calculated

This project has received funding from the EU H2020 research and innovation programme under Grant Agreement No 678396

here using the relationship between *in situ* measurements of DFM and flesh weight from an extensive French database of oyster growth monitoring, the *Réseau d'observations conchylicoles* (RESCO; $R^2 = 0.83$, $p < 0.001$), applied to DFM output from the model.

As these indicators depend on user-defined weight thresholds or dates of interest, these can easily be adapted to those of specific interest to a given user. For example, here we considered the timing of the main French market, which is early December, coinciding with the cultural tradition of eating oysters around Christmas. However, the secondary summer market may also be of interest, or may be the primary market elsewhere, and modifying the date range in transforming the growth data to the indicator would provide insight specific to this case (e.g., mapping total weight on July 15 rather than December 1) and is easily achieved. Similarly, we considered the minimum market weight threshold (30 g) here for adult oysters, and the T25 (14 g) threshold for spat resale, but a producer may be interested in heavier calibre adult or a different spat size to suit their infrastructure, production cycle, or markets, and the defined weight can be changed in producing the indicator.

Closeups of adult weight on December 1 for several "hot spot" regions are presented in Fig. 4.7, and reveal a high degree of regional spatial variability in indicator results over distances of only ~100km. For example, modelled weight for the area around Bourgneuf Bay, France, is approximately 40 g for this indicator and scenario, but only approximately 25 g just 100 km further northwest in South Brittany (Fig. 4.7c). More extreme is the example off the west coast of Africa (Fig. 4.7d), where modelled weights of > 55 g are less than 100 km from modelled weights < 15 g. This demonstrates the use of such indicators to both highlight broad regions of potential interest for aquaculture development, but also the potential to target sites of interest for further investigation within these regions. Several areas identified as having good offshore growth potential are in reasonably close proximity to areas wherein Pacific oyster cultivation currently takes place (e.g., the French Atlantic coast, around Scotland), albeit in the more nearshore coastal bays, estuaries, and fjords. This pre-existence of a shellfish industry, and Pacific oyster cultivation in particular, would be expected to facilitate an adjacent transition to the offshore environment, although major differences in production between the two environments – near- and offshore – are also expected. Likewise, certain areas where shellfish cultivation, including the European flat oyster (*species*), take place (e.g., the North Sea and its transitional waters with the Baltic Sea (Kattegat, Belt Sea)) have been mapped as having high Pacific oyster growth potential. In such areas, industry diversification to include Pacific oyster production would also likely be facilitated in many ways though existing related industry, but may not be desirable as competition between species may have a deleterious effect on the pre-existing industry (e.g., colonization of flat oyster aquaculture structures by Pacific oyster if in too close proximity). Further areas of high growth potential, where industrial shellfish aquaculture is not currently practiced, notably off the west coast of Africa, may suggest areas where new activity would be worth investigating.

This project has received funding from the EU H2020 research and innovation programme under Grant Agreement No 678396

Table 4.4. Example indicators produced here for each production cycle stage.

Production stage	**Indicator**
Spat pre-grow	Time to reach T20/T25 (14 g)
Adult grow-out	Time to reach market weight (30 g)
	Total weight on December 1
	Number of spawning events
Finishing/fattening	Quality index

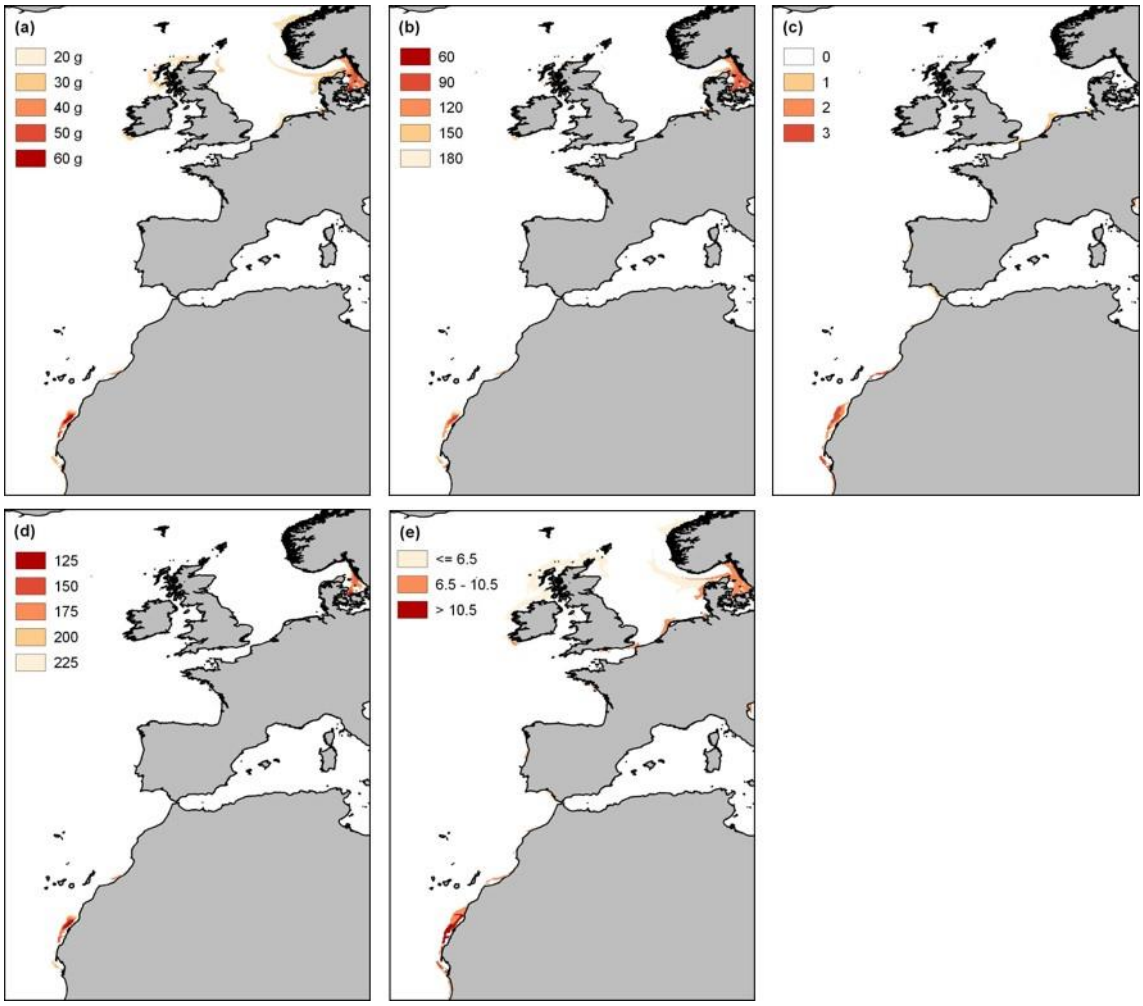

Figure 4.6. Example indicators detailed in the text and summarized in Table 4.4, applied to modelling for the early century reference period (2000-2004); (a) adult total weight (g) on December 1, (b) days until adults reach 30g, (c) number of spawning events per year, (d) days until spat reach 14g, and (e) quality index (%) associated with *Normale* (<6.5%), *Fine* (6.5-10.5%), and *Spéciale* (>10.5%) classes. White areas were masked by thresholding criteria detailed in Table 4.3.

This project has received funding from the EU H2020 research and innovation programme under Grant Agreement No 678396

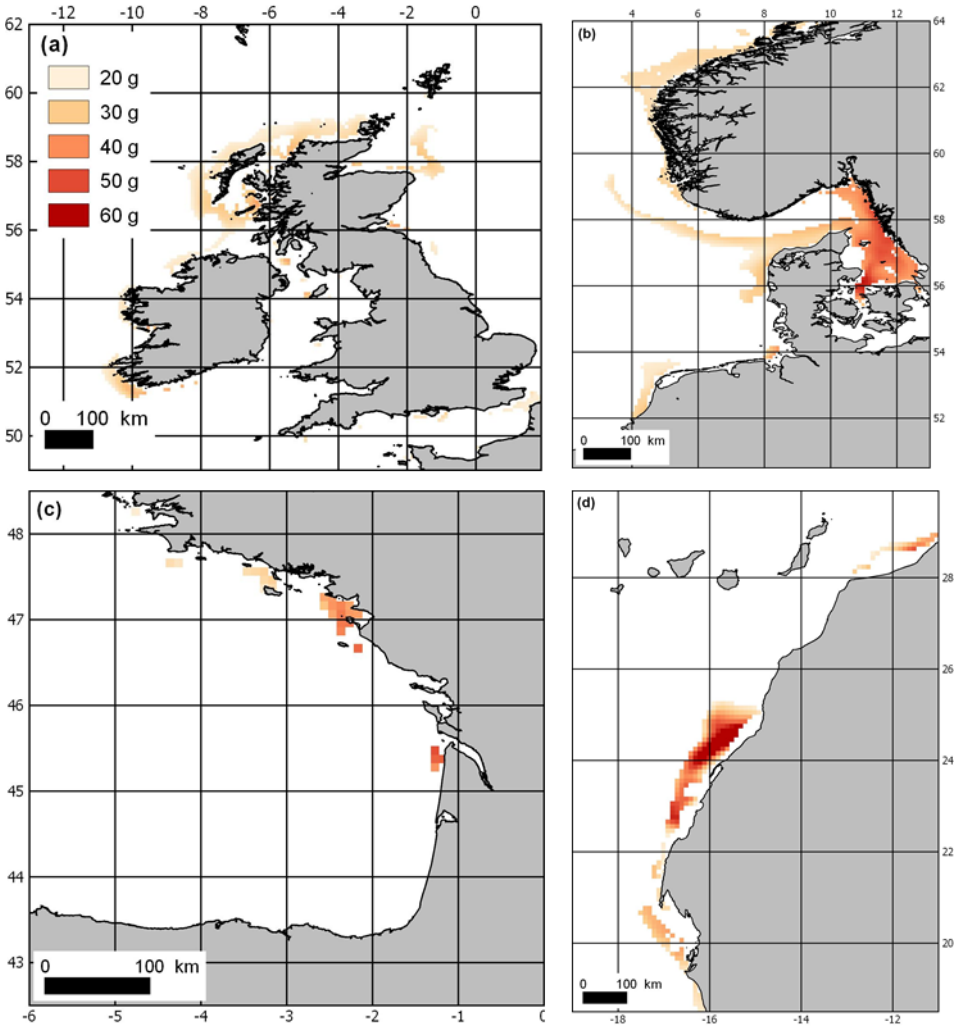

Figure 4.7 Closeups of adult total weight (g) on December 1 for the early century reference period (2000-2004) for (a) the UK and Ireland, (b) the North Sea and Baltic transitional waters, (c) the French Atlantic, and (d) the northwestern African coast. White areas were masked by thresholding criteria detailed in Table 4.3.

4.4. Highlights of Pacific oyster aquaculture sustainability across Europe under changing climate scenarios

In addition to the application of the aquaculture indicators described and demonstrated via mapping in the previous section for early century conditions, an increasingly important consideration in related policy, investment, and development decision making has to do with future climate change. Although increased sea surface temperature and decreased net primary productivity are generally expected under warming scenarios, changes to our climate system, and the effects and feedbacks thereof on a broad range of biogeochemical processes and ecosystems, are highly complex and associated with a high degree of uncertainty. To begin to address this in terms of oyster aquaculture indicators, the biogeochemical variables used to model Pacific oyster growth were modelled for two distinct future climate change

This project has received funding from the EU H2020 research and innovation programme under Grant Agreement No 678396

scenarios in addition to an early century reference period which benefitted from observation data assimilation: a “business as usual” scenario, whereby greenhouse gas emissions reach and exceed 8.5 W m^{-2} by the end of the century, and one whereby emissions level off to 4.5 W m^{-2} by the end of the century (Moss et al., 2010). By assessing and comparing these two distinct future scenarios, we can begin to constrain and assess the potential uncertainty expected in future oyster growth potential and associated industry indicators. It should, however, be acknowledged, that we use a combination of three models (climate change, POLCOMS-ERSEM, and DEB), with each model being associated with its own inherent uncertainty, and therefore propagate the uncertainties in the final results.

In addition to areas that have good current potential or are current “hot spots”, areas that are expected to remain stable in terms of growth potential projections, or even to increase under projected climate conditions can then be targeted. Alternatively, areas where growth potential is expected to decrease can be avoided. Furthermore, areas of stable or increasing growth potential under multiple contrasting climate scenarios, as assessed here, have the advantage of being more climate robust. In other words, the uncertainty associated with future climate conditions and their effects on crucial biogeochemical variables is found to affect growth potential less in these areas. Figure 3.8 outlines the series of steps and decisions that can be taken using the mapped indicators to highlight areas of interest to be prioritized for further exploration of aquaculture activity. First, areas that can be considered to have good potential under the baseline condition are identified using a user-defined criterion. In this case, the minimum market size threshold (30 g) is applied to the maps of total adult weight on December 1; areas where oysters are modelled to reach or exceed 30 g by this date are retained for the next step. Then, areas that will also achieve this “good” status in any future scenario are retained. Finally, consistency between future scenarios is considered in terms of climate robustness, as described above; here, this is the absolute difference between the two future scenarios normalized to the indicator value itself (eq. 1). Areas that achieve all of these criteria are of high priority.

$$|RCP\ 8.5_{indicator} - RCP\ 4.5_{indicator}| / \max(RCP\ 8.5_{indicator},\ RCP\ 4.5_{indicator}) \qquad \text{eq. 1}$$

This project has received funding from the EU H2020 research and innovation programme under Grant Agreement No 678396

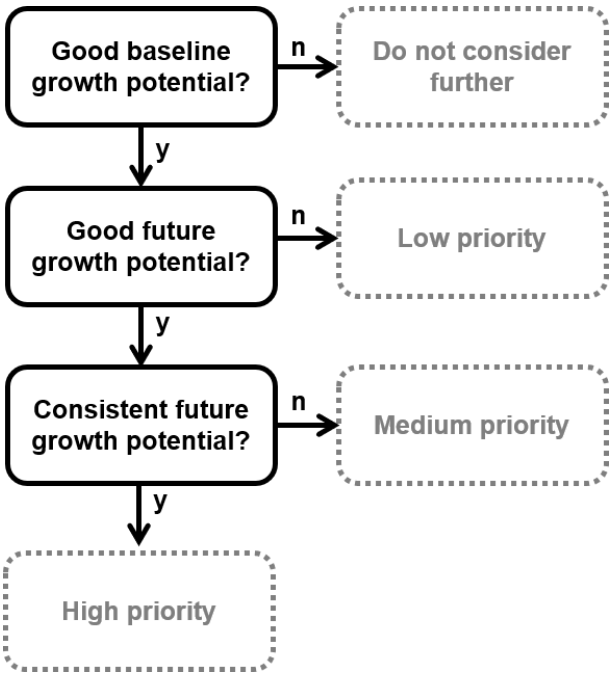

Figure 4.8. Schematic of aquaculture indicator mapping used in a decision support system to identify high-priority regions for further offshore aquaculture consideration.

In Fig. 4.9, currently promising areas (panel (a); i.e., the first step in Fig. 4.8), as well as the extents that are also promising in the future and their climate robustness (panel (b))) are mapped. The example regions from Fig. 4.6 are similarly mapped in greater detail in Figs. 4.10-4.13. Within each of these, the total weights are extracted from a smaller area (black squares in panel (b) of each) for each of the early and late century scenarios for further consideration (Fig. 4.14).

This project has received funding from the EU H2020 research and innovation programme under Grant Agreement No 678396

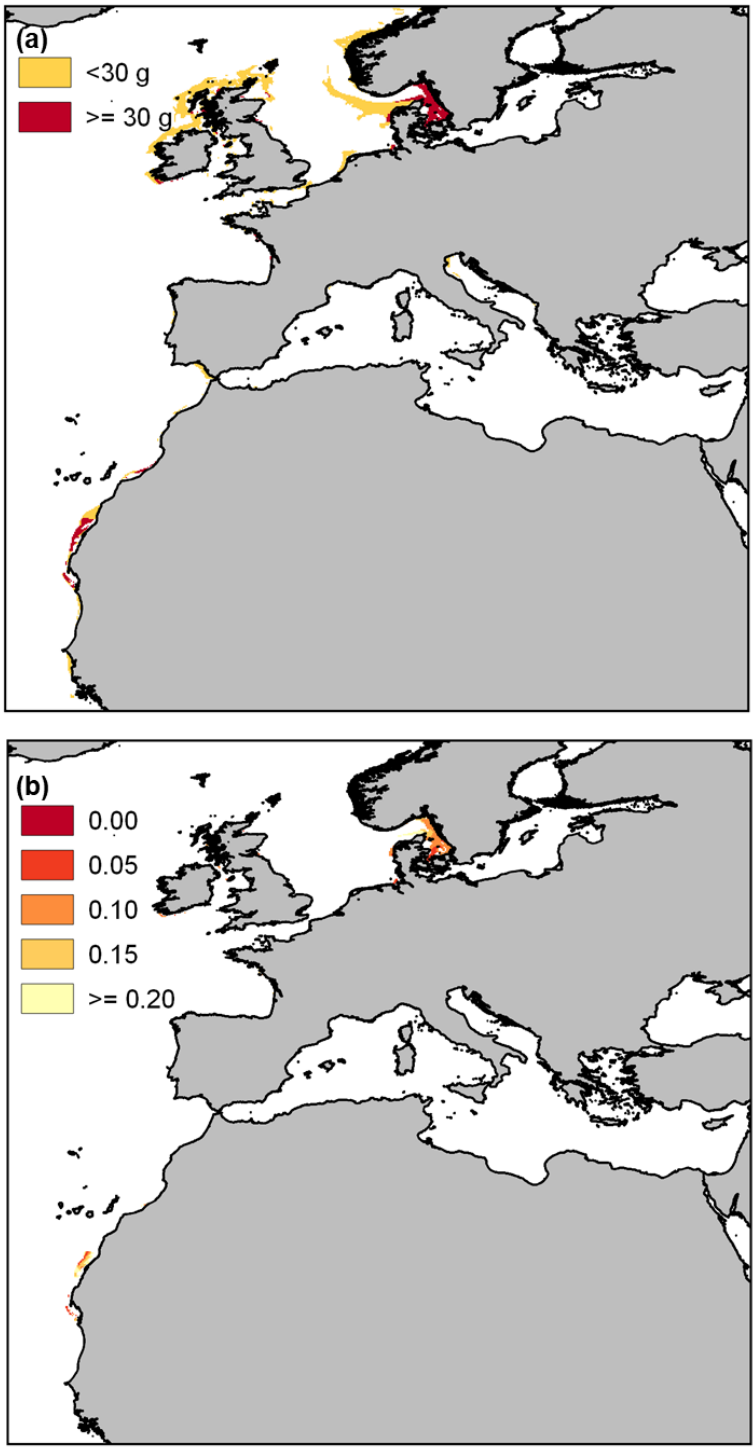

Figure 4.9. (a) Areas of current "good" growth potential within the full model domain, defined here as total adult weight reaching or exceeding 30 g by December 1 (dark red), and (b) climate robustness (weight-normalized absolute difference in future scenario-projected growth (eq. 1)) mapped for areas of good current and future growth potential. Darker red areas are considered to be more climate robust.

This project has received funding from the EU H2020 research and innovation programme under Grant Agreement No 678396

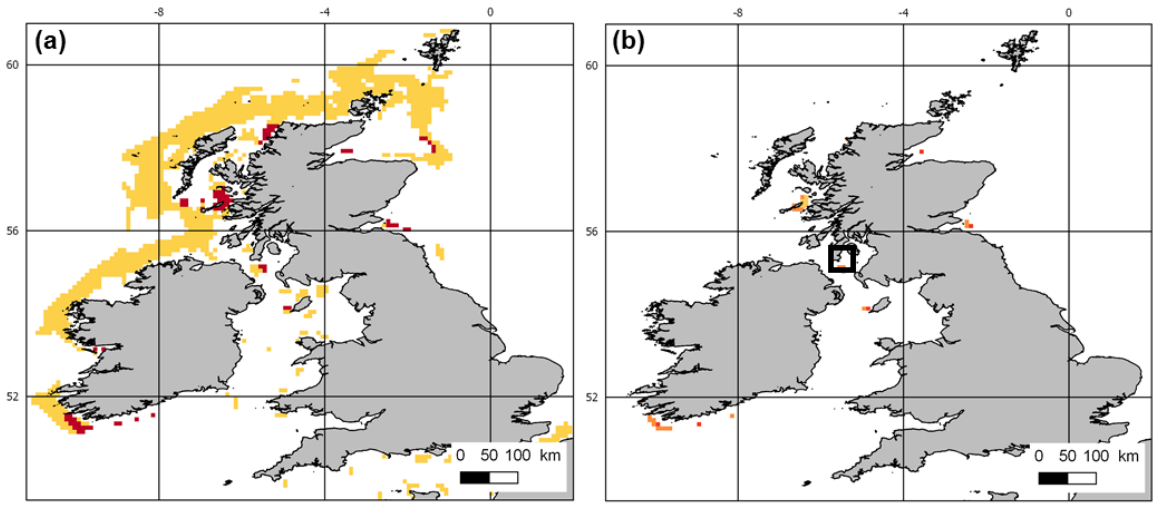

Figure 4.10. (a) Areas of current "good" growth potential within the UK and Ireland, defined here as total adult weight reaching or exceeding 30 g by December 1 (dark red), and (b) climate robustness (weight-normalized absolute difference in future scenario-projected growth) mapped for areas of good current and future potential. Colour scales are as in Fig. 4.9. The black square in (b) indicates the area analyzed in Fig. 4.14.

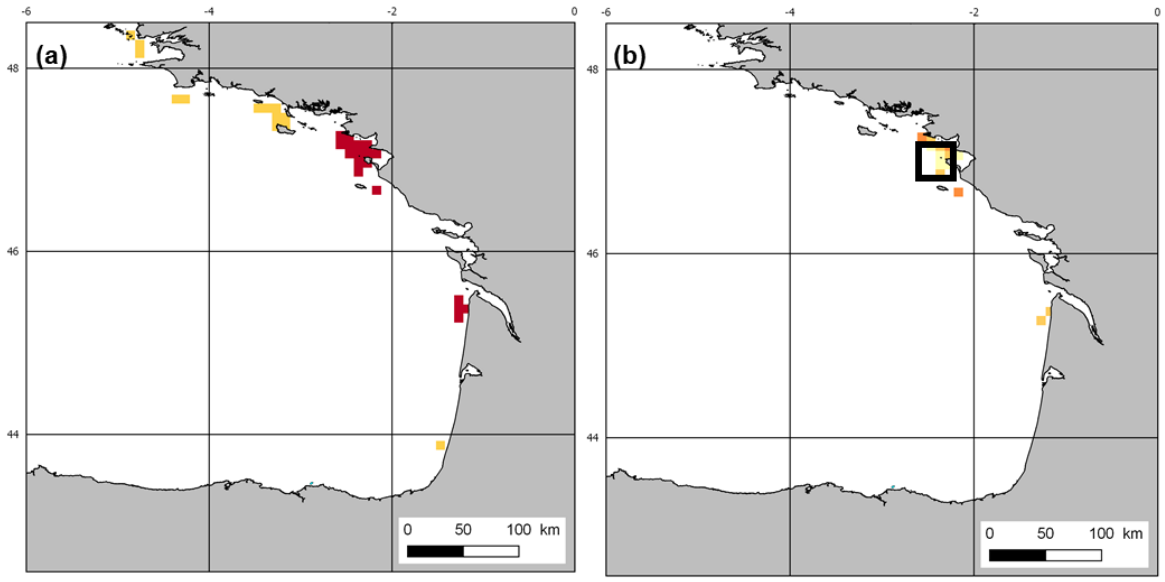

Figure 4.11. (a) Areas of current "good" growth potential for the French Atlantic, defined here as total adult weight reaching or exceeding 30 g by December 1 (dark red), and (b) climate robustness (weight-normalized absolute difference in future scenario-projected growth (eq. 1)) mapped for areas of good current and future potential. Colour scales are as in Fig. 4.9. The black square in (b) indicates the area analyzed in Fig. 4.14.

Additional areas of interest for future shellfish aquaculture activities may be highlighted by superimposing infrastructural considerations that are necessary for or which may open up new avenues for cultivation upon the maps of current and future climate-robust growth potential. This may be considered in either of two ways: existing or planned infrastructure may be used to constrain broader areas of interest from a growth potential perspective. Or, areas of exceptional biological potential, but with limited infrastructural resources, may be targeted in

This project has received funding from the EU H2020 research and innovation programme under Grant Agreement No 678396

planning for major infrastructural investments in support of aquaculture. For example, in Fig. 4.12 the limitation to aquaculture development of port access in areas of high oyster growth potential in western Africa is contrasted with the European situation. A given area should be within 25 nm of a port to warrant aquaculture activity development, in terms of cost-effectiveness (Kapetsky et al. 2013). To leverage observed potential in western Africa, developments in the aquaculture industry could proceed within the area where 25 nm to a port overlaps with high growth potential (e.g., Fig. 4.12c-i). Mapped areas of exceptionally high growth potential could also be used as part of the discussion around where to situate new ports (e.g., Fig. 4.12c-ii). The potential for offshore co-production of shellfish and wind energy has also received considerable attention over recent decades (Buck and Langan, 2017), particularly in the North Sea, where the offshore wind energy sector is both well-established and continues to develop. Essentially, the presence of wind farm platforms is leveraged to suspend longlines or floating cages for oyster or mussel cultivation, providing added-value to the initial platform investments within an integrated coastal management framework (Buck and Langan, 2017). In Fig. 4.13a, the locations of operational, under construction, and authorized wind farms since 2015 are superimposed on areas of current interest in the North Sea, in terms of growth potential, and on climate robust growth potential areas Fig. 4.13b. Several resulting priority areas, with high current growth potential that is expected to remain stable, are highlighted.

This project has received funding from the EU
H2020 research and innovation programme
under Grant Agreement No 678396

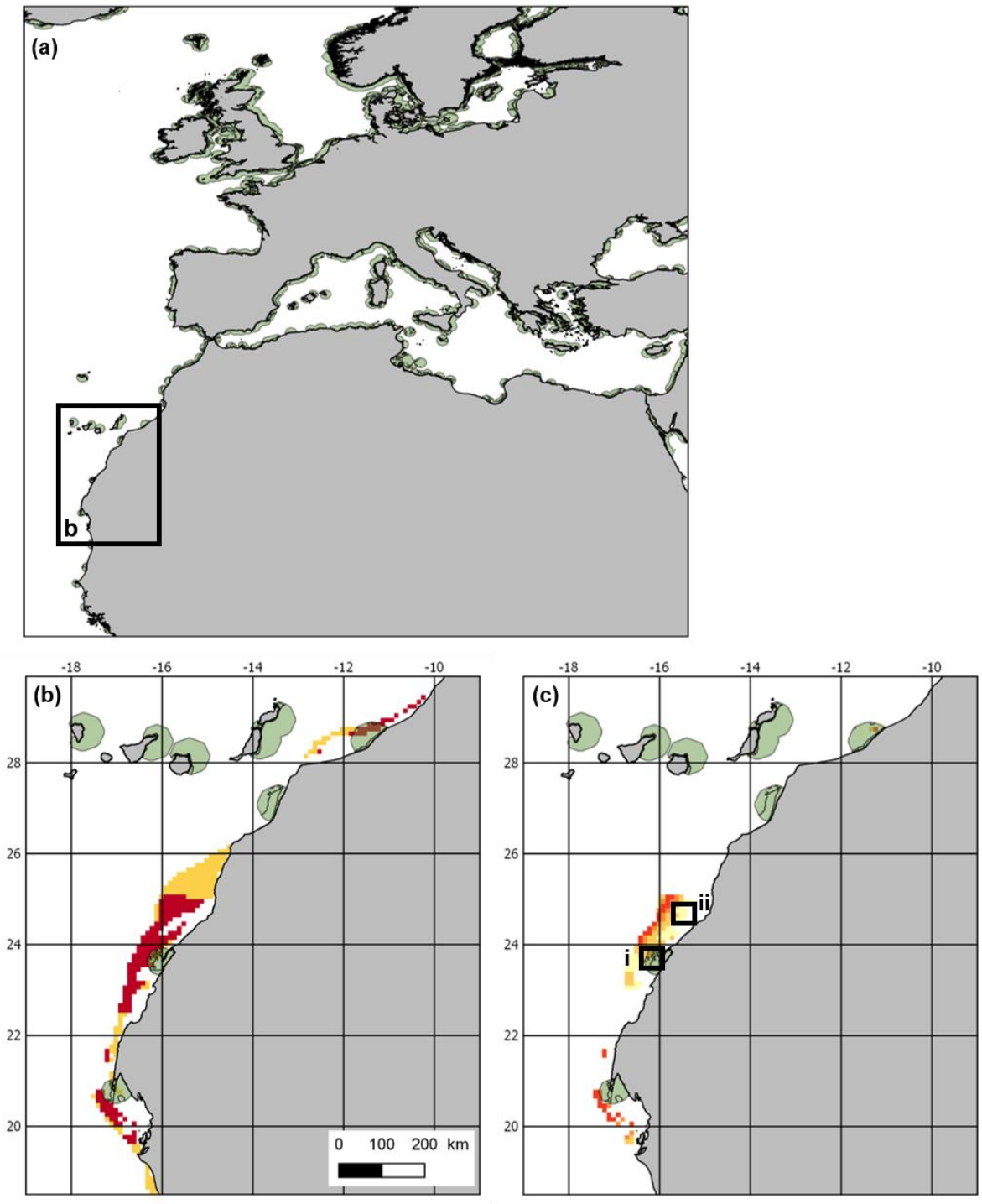

Figure 4.12. (a) 25 nm distance to a port for the full model domain considered here (green area along coasts). (b) Areas of current "good" growth potential for Western Sahara, defined here as total adult weight reaching or exceeding 30 g by December 1 (dark red), and (c) climate robustness (weight-normalized absolute difference in future scenario-projected growth (eq. 1)) mapped for areas of good current and future potential. Colour scales are as in Fig. 4.9. The black squares in (c) indicate the areas analyzed in Fig. 4.14. Areas within 25 nm of existing ports are superimposed on indicator maps in (b) and (c) (green shading).

This project has received funding from the EU H2020 research and innovation programme under Grant Agreement No 678396

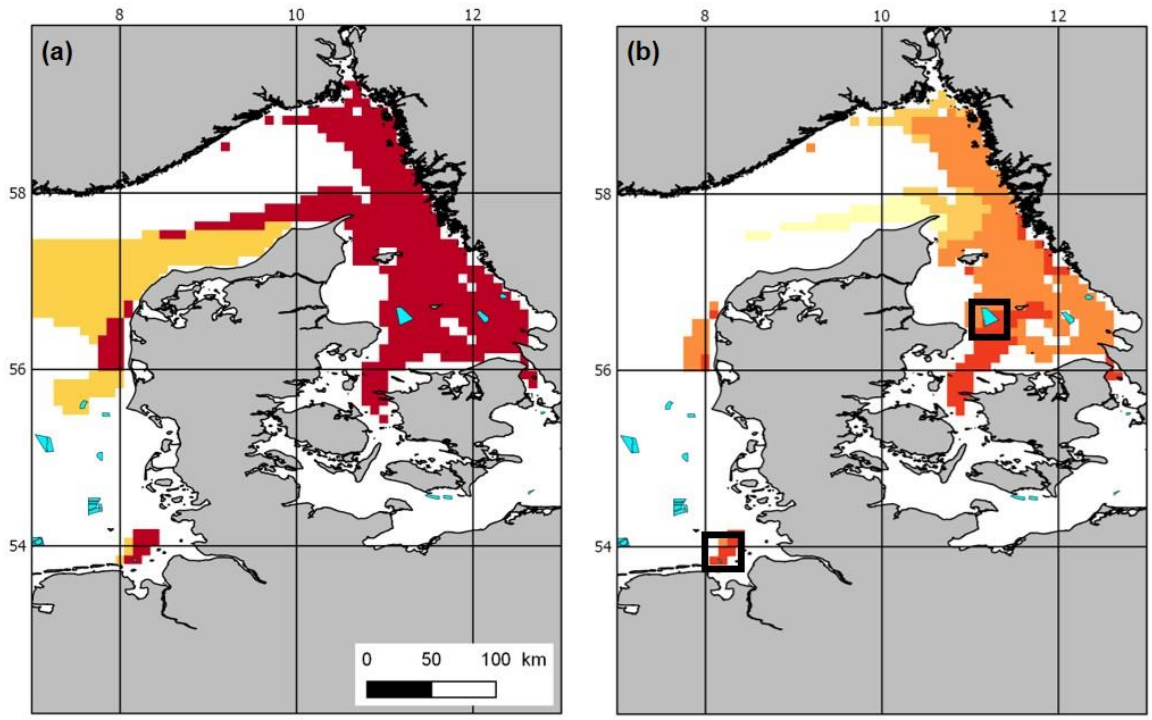

Figure 4.13. (a) Areas of current "good" growth potential for the North Sea-Baltic transitional waters (Kattegat; Belt Sea), defined here as total adult weight reaching or exceeding 30 g by December 1 (dark red), and (b) climate robustness (weight-normalized absolute difference in future scenario-projected growth (eq. 1)) mapped for areas of good current and future potential. Colour scales are as in Fig. 4.9. The black squares in (b) indicates the area analyzed in Fig. 4.14 (Kattegat, Nordergrunde). Here, the locations of wind farms that are operational, under construction or authorized since 2015 are superimposed (blue polygons).

The current modelling and mapping exercises, considering (i) Pacific oyster tolerance ranges with regards to several biogeochemical variables and (ii) DEB-modelled Pacific oyster growth potential indicators, both under various climate change scenarios, as well as (iii) examples of technical infrastructural constraints and opportunities, highlights the utility and added spatial nuance possible to achieve through our approach. The results could be extended through more complete Spatial Multi-Criteria Analysis, incorporating additional socio-economic factors that further influence whether cultivation at a given site would be possible or that may hinder or be leveraged to the benefit of aquaculture. This is especially relevant as many regions and countries undertake or update Marine Spatial Planning, for which such spatial information is crucial. Although different oyster growth scenarios were produced, under varying future climate scenarios, there is also uncertainty in future conditions for many other issues that would affect the development, sustainability, and success of aquaculture, including changes to fisheries management. Furthermore, not all factors that would be expected to influence oyster biological growth potential are included in the modelling and constraint mapping here. For example, ocean acidification is expected to increase under all climate change scenarios, and to have a substantial impact on the ability of shellfish to thrive (Kroeker et al., 2010; Barton et al., 2012).

This project has received funding from the EU H2020 research and innovation programme under Grant Agreement No 678396

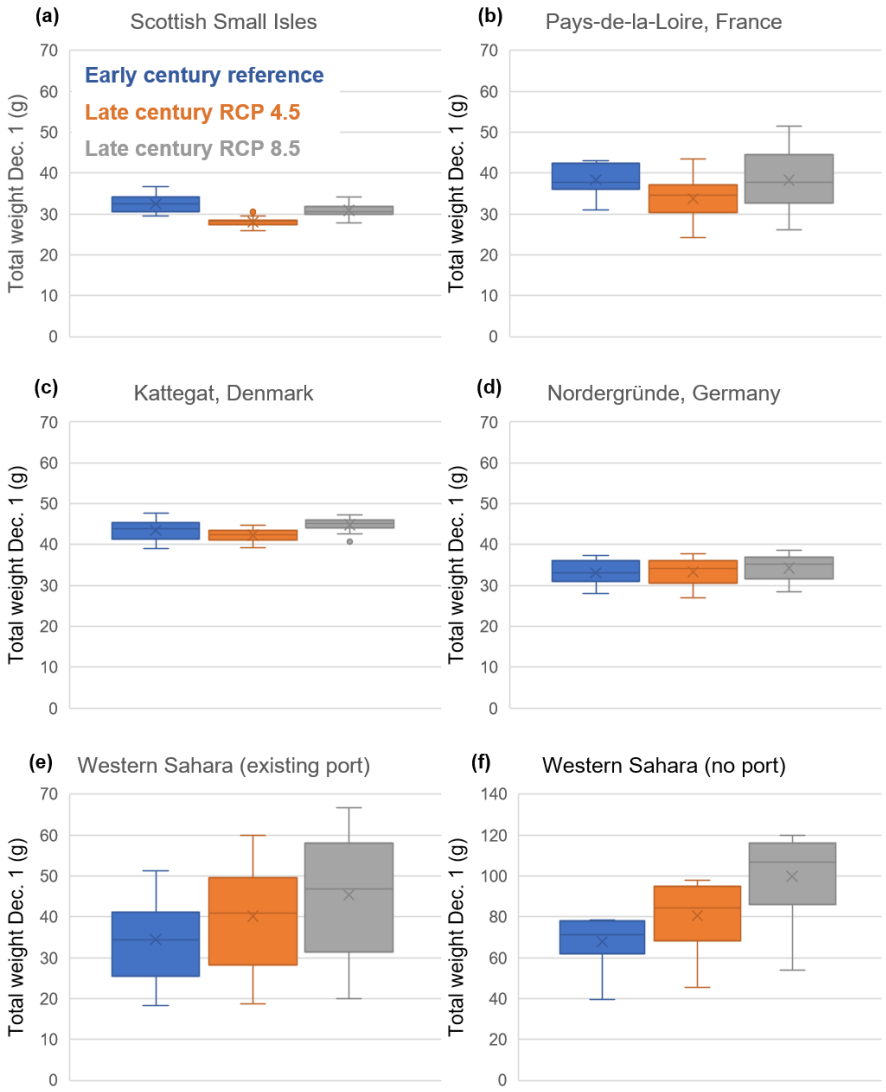

Figure 4.14. Comparison of Pacific oyster growth potential for early century baseline (blue) and two future climate scenario projections, RCP 4.5 (orange) and RCP 8.5 (grey), for example areas within several identified areas of interest.

A valuable approach for integrating modelled data in support of aquaculture decision making is demonstrated, with important limitations and avenues for future work identified. With the availability of *in situ* data for DEB model calibration and validation, this approach could be used for other species of interest too (e.g., blue mussel (*Mytilus edulis*)). For Pacific oyster, *C. gigas*, a suite of industry-relevant indicators for current growth potential and future, climate-related sustainability was proposed. Several broad regions of current and future interest were highlighted, within which more localized site selection and opportunities to leverage existing or to plan for future infrastructure were demonstrated. Results at this spatial scale are also expected to inform decisions on where more detailed investigation and modelling would be most beneficial.

This project has received funding from the EU H2020 research and innovation programme under Grant Agreement No 678396

5. Assessing the impact of aquaculture waste on environmental status in an eastern Mediterranean Allocated Zone for Aquaculture (AZA) using Aquaculture Integrated Model (AIM).

5.1. Background

The input of dissolved inorganic nutrients from fish farms may affect the ecological regime of the surrounding areas (Sara, 2007ab). The dispersion of waste largely depends on the hydrography in the vicinity of the fish farms, with effluents often being accumulated at significant distances from the farms (Tsagaraki et al., 2011). Consequently, planning and licensing of cage aquaculture can be complex, particularly in Allocated Zones for Aquaculture (AZAs) with potential cumulative impacts from multiple farms. Decision makers therefore need help to assess if a site is suitable for cages and to determine acceptable biomass limits. Coupled physical–biogeochemical numerical models can be used to examine the impact of the fish farms on the marine ecosystem of the surrounding areas, offering a low-cost solution, as compared with systematic *in situ* monitoring. More importantly, they can be used, through a series of scenario simulations, as management tools in order to obtain a sustainable and efficient spatial planning of the fish farms, considering the area carrying capacity and the overall effect on the ecosystem.

5.2. Description & limitations of the modelling approach

The Aquaculture Integrated Model (AIM; Tsagaraki et al., 2011; Petihakis et al., 2012) was used in an AZA (Vourlias Bay, Greece) to examine the fate of seabass/seabream aquaculture wastes under different scenarios (e.g., fish production, changing climate) and assess their potential impacts on the surrounding ecosystem, in terms of good environmental status (see *TAPAS* D5.3 for a more detailed description). The modelling tool consists of a high-resolution 3D coupled hydrodynamic/biogeochemical model, with a mass balance model (Tsapakis et al., 2006) used to calculate nutrient inputs from the fish cages, based on fish feed data. A series of nested models is used to consistently downscale the hydrodynamics and biogeochemistry from the coarser resolution (~3 Km) model of the wider area (Aegean) to the high-resolution model (~50m) of the fish farm area. The model was validated against available satellite (Chl-a) and collected *in situ* (Chl-a, nutrients, mesozooplankton) data. The model produces maps of near surface currents, Chl-a, and dissolved inorganic nutrients (phosphate, nitrate, ammonium, silicate) that can be used to calculate environmental indicators (i.e., environmental index; Primpas et al., 2010) describing the environmental status of the area and assess the AZA carrying capacity.

This project has received funding from the EU H2020 research and innovation programme under Grant Agreement No 678396

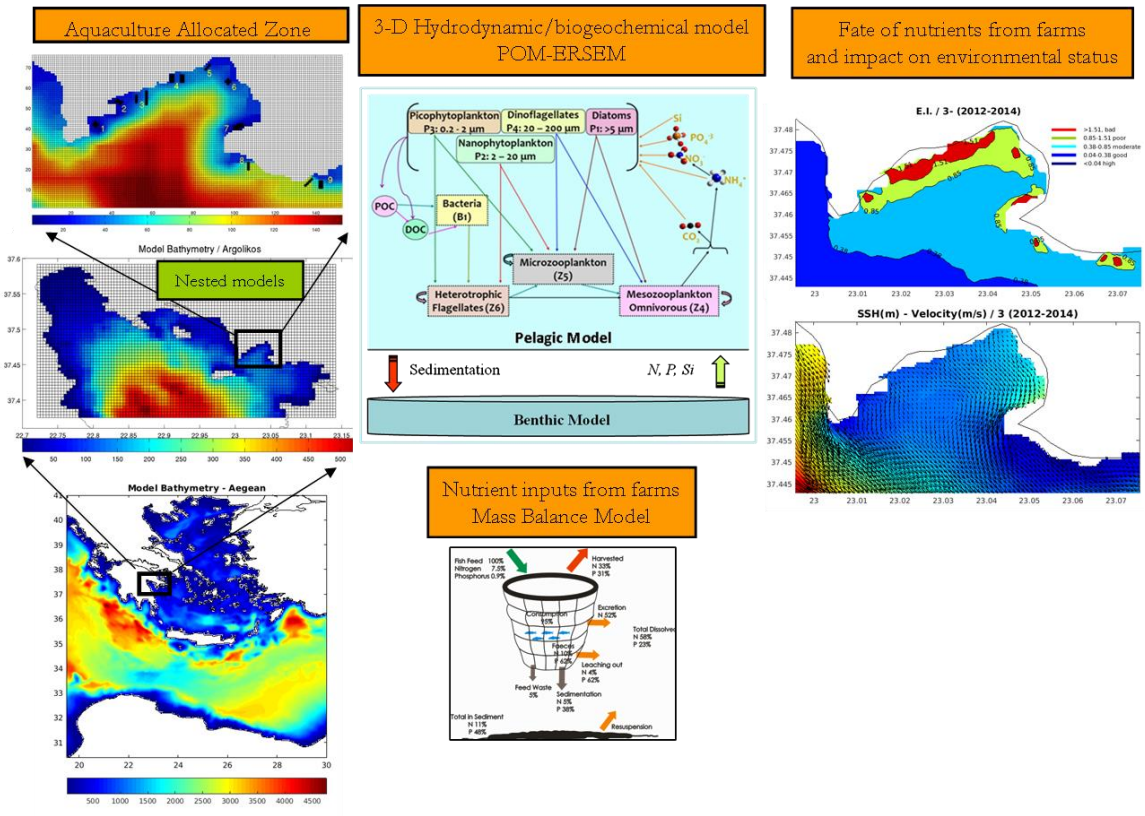

Figure 5.1. Aquaculture Integrated Model schematic, showing the series of nested models (Aegean/3Km resolution, Argolikos Gulf/500m resolution, Vourlias bay/50m resolution) on the left, the biogeochemical and mass balance model schematics on the middle and an example of AIM model output (Environmental status index and currents) on the right panel.

The use of a comprehensive biogeochemical model, such as ERSEM allows the complex food web response, triggered by the nutrient inputs, to be investigated. The high resolution (~50m) of the hydrodynamic model and its progressive downscaling through nesting with coarser models allows a realistic simulation of circulation, which is crucial for the correct dispersion of aquaculture effluents.

The main prerequisite for the initial model setup is a relatively high-resolution bathymetry of the area and initial fields for the hydrodynamic (temperature, salinity) and biogeochemical (dissolved inorganic nutrients) models that are usually obtained from coarser regional-scale models (e.g., of the Aegean Sea) and/or existing climatologies. In addition, fish feed data are also required to calculate fish farm wastes. The main limitation of the modelling system is that it is computationally very demanding, (e.g., two days for a one-year simulation in a 40-CPU server), mainly due to the very high resolution of the near-field model. Moreover, *in situ* measurements (inorganic nutrients, Chl-a, currents), needed for a more detailed model validation, may require some additional cost and effort for the tool application. We should note that a realistic simulation of circulation on such local scale, without employing any data assimilation, is rather challenging (see *TAPAS* D5.3), as small-scale coastal features are largely driven by the larger scale circulation, obtained through the open boundary nesting with the coarser model. Data assimilation (e.g., satellite altimetry) in the coarser model, or even in the fine-scale model if high-resolution data are available, is expected to further improve the model precision. The uncertainty of coastal hydrodynamics is even higher in future climate

This project has received funding from the EU H2020 research and innovation programme under Grant Agreement No 678396

simulations, as the climate forcing obtained from relatively coarser atmosphere-ocean models is less relevant at coastal scales.

5.3. Aquaculture indicators

The tool has been implemented to assess the current environmental impact of the fish farms in the Vourlias AZA (Argolikos Gulf, Greece) and to investigate the system carrying capacity through additional scenarios adopting an increased fish production. The tool was also implemented to investigate the potential changes in the AZA environmental status due to changing climate conditions (i.e., increase of temperature/stratification, etc.), under future scenarios for the 2030-2050 and 2080-2100 time-windows. The environmental status was assessed calculating the Environmental Index (E.I., Primpas et al., 2010), using the model simulated nutrients and Chl-a concentration:

$$E.I.=0.279*PO4 + 0.261*NO3+ 0.296*NO2+ 0.275*NH4+ 0.214*Chl\text{-}a$$

and the following environmental scaling: <0.04 very good, 0.04 - 0.38 good, 0.38 - 0.85 moderate, 0.85 - 1.51 poor, > 1.51 bad.

The environmental conditions in the AZA were found to be “good” during the well-mixed winter period and “moderate” to “poor” during more stratified summer periods (see Figure 5.2). The environmental conditions in the vicinity of different fish farms were found to be correlated to the fish farm production and the predominant current speed, with some fish farms characterized by relatively better environmental conditions, despite their high fish production due to the stronger prevailing currents that result in the more efficient off-shore dispersion of fish farm wastes (see *TAPAS* D5.3). A scenario simulation, adopting a doubled fish production was performed, investigating the carrying capacity of the AZA. An additional increased production scenario was also performed, distributing this increase based on the environmental index variability, thus allocating more production increase in fish farms characterized by better conditions. In this case the deterioration of conditions in fish farms was more balanced, avoiding extremes (i.e., fish farms #3, #4; Figure 5.3).

This project has received funding from the EU H2020 research and innovation programme under Grant Agreement No 678396

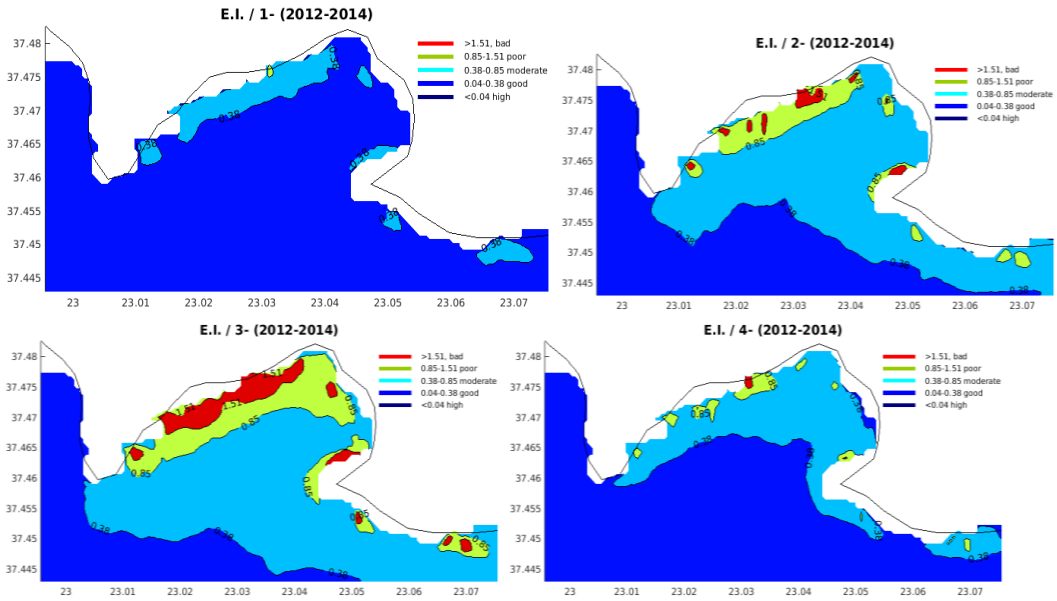

Figure 5.2. Seasonal variability (1=winter, 2=spring, 3=summer, 4=autumn) of simulated environmental index over the 2012-2014 period.

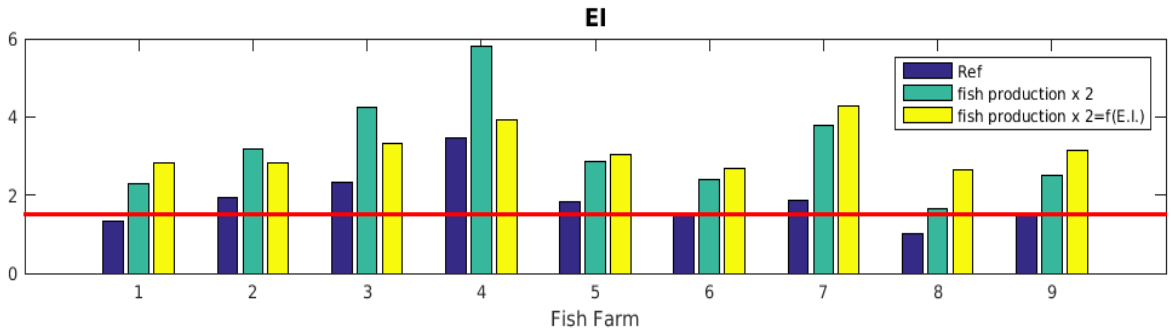

Figure 5.3. Mean 2013 simulated summer environmental index (E.I.) in the vicinity of the fish farms, comparing reference fish production, doubled fish production, and doubled fish production distributed across different fish farms taking initial E.I. variability into account. The red line indicates the E.I. threshold identifying "poor" environmental conditions (1.51).

For the future climate simulations, the model was forced with climatic atmospheric forcing (obtained from the Swedish Meteorological Hydrological Institute), while open boundary conditions (temperature, salinity, inorganic nutrients) were obtained from PML Mediterranean basin scale future climate simulations (Kay and Butenschon, 2018), adopting an "anomaly" approach (i.e., multiply the open boundary conditions of the hindcast simulation with a changing factor, future/present, obtained from PML boundary conditions).

Future climate conditions were mostly characterized by an increase in temperature (from +0.4ºC in 2030 under RCP 4.5 to +2ºC in 2080 under RCP 8.5), resulting in a slight decrease in plankton biomass due to their increased metabolism (Figure 5.4), and an increase in open sea dissolved inorganic nutrients (obtained from the basin scale model). The latter is probably

This project has received funding from the EU H2020 research and innovation programme under Grant Agreement No 678396

due to the significant increase of open sea salinity predicted by the basin scale model, which results in increased winter mixing and nutrient enrichment. Overall, changes in the environmental status under future climate conditions were relatively small, as compared to present conditions (Figs 5.4-5.6) and were related to the combined effect of increased open boundary dissolved inorganic nutrients, the increased plankton metabolism, and the effect of changing stratification on the dispersion of aquaculture wastes.

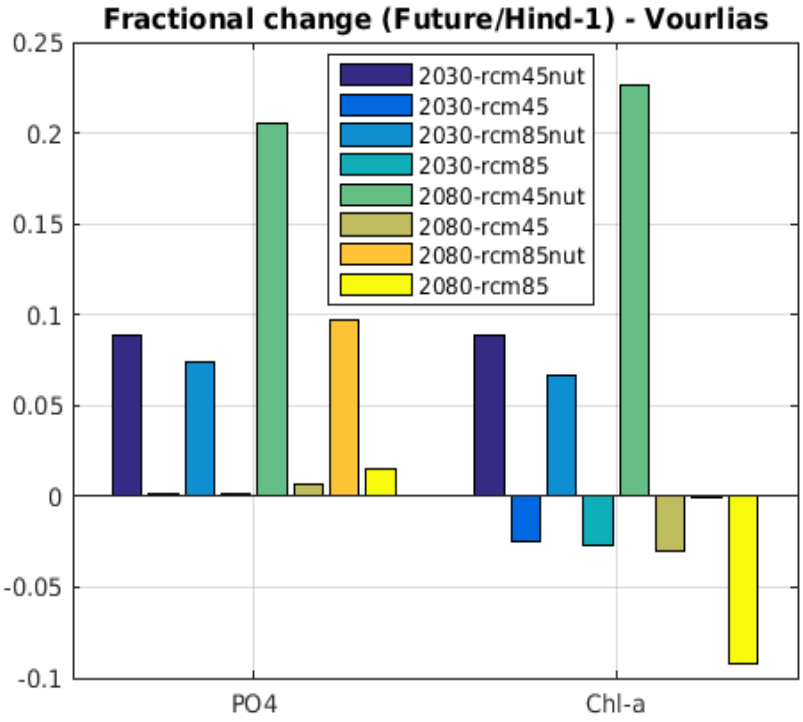

Figure 5.4. Mean summer fractional change (Future/present-1) of simulated average phosphate and Chl-a under future climate scenarios (2030-2050 & 2080-2100 rcm4.5 and rcm8.5), adopting temperature, salinity and dissolved inorganic nutrients (e.g. 2030-rcm45nut) or just temperature and salinity from the boundary conditions of the basin scale model. The decrease in Chl-a in the second series of experiments is related to the increased metabolism, resulting from temperature increase.

This project has received funding from the EU H2020 research and innovation programme under Grant Agreement No 678396

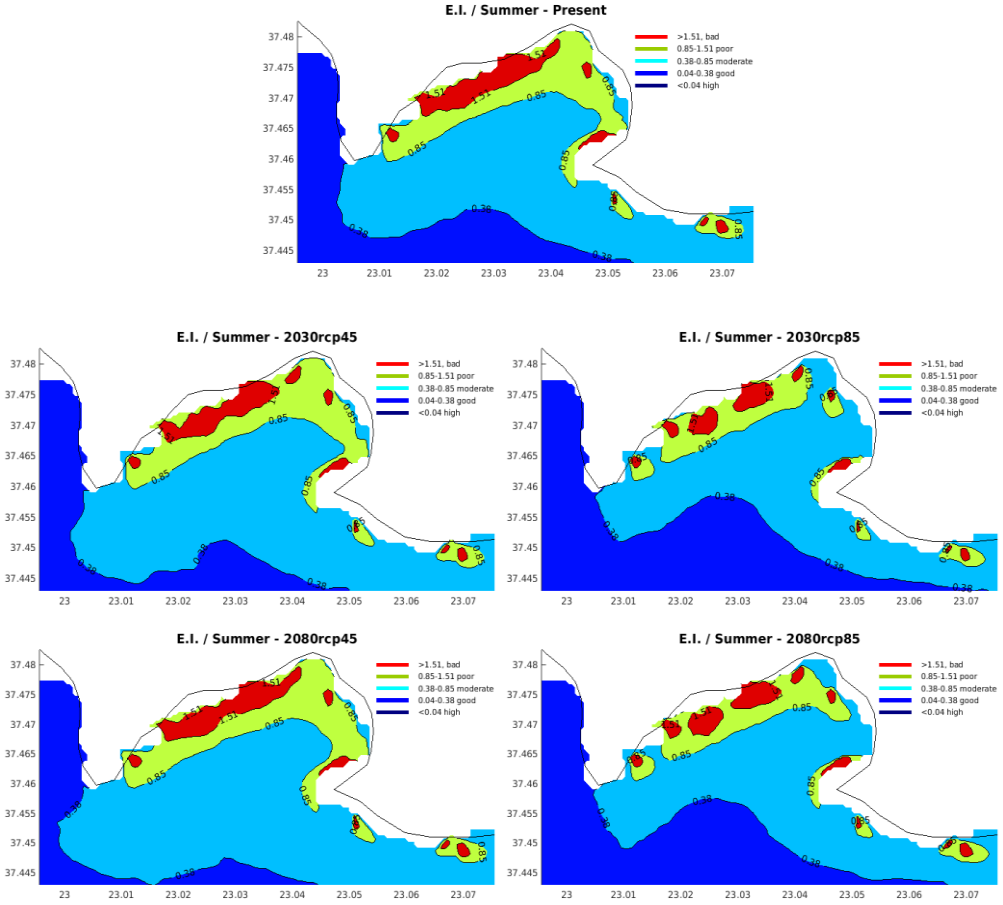

Figure 5.5. Mean simulated summer environmental index under present and future climate (2030-2050 & 2080-2100 RCP 4.5 and RCP 8.5) conditions.

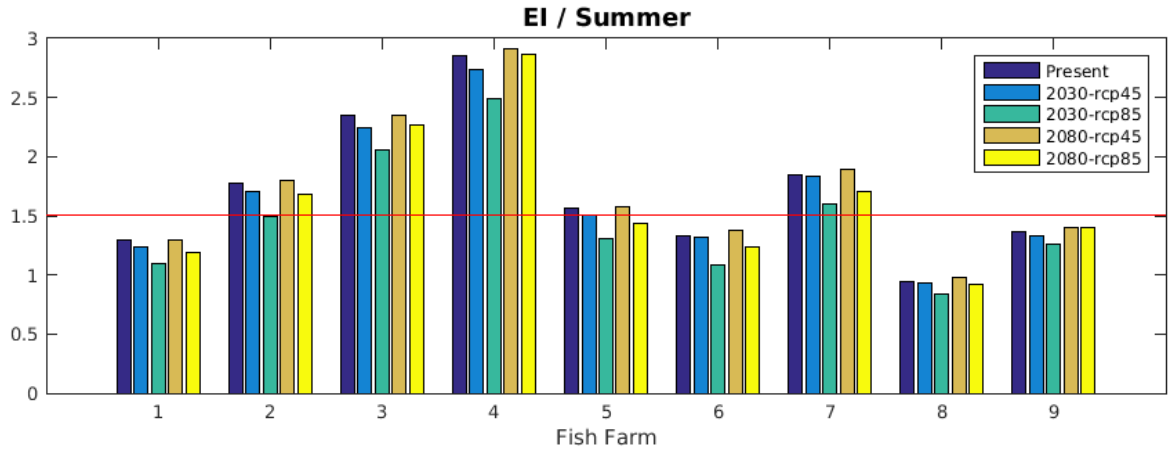

Figure 5.6. Mean summer environmental index in the vicinity of fish farms under present and future climate (2030-2050 & 2080-2100 RCP 4.5 and RCP 8.5) conditions.

This project has received funding from the EU H2020 research and innovation programme under Grant Agreement No 678396

5.4. Summary of Mediterranean finfish aquaculture environmental impacts under changing climate and exploitation scenarios

Once setup and validated, AIM can be used to examine the impact of single or multiple (e.g., AZA) existing aquaculture units in terms of environmental status, using the model output (e.g., Chl-a, inorganic nutrients, oxygen) to calculate environmental indices (e.g., Primpas et al., 2010). More importantly, it can be used to simulate different scenarios (e.g., comparing farm locations, level of production) as a management tool for the spatial planning and licensing of new farms or the increase of production for existing farms, providing decision support for government authorities and producers.

The use of a comprehensive biogeochemical model, such as ERSEM, allows the complex food web response, triggered by the nutrient inputs, to be investigated. Currently, a first order simple benthic model is used, calculating the nutrient fluxes from the sediment. A further model development would be to implement the full ERSEM benthic model that would allow the effect of uneaten food and wastes from the fish cages to the underlying benthic ecosystem to be simulated, calculating a series of benthic indexes. This would however require some additional effort and cost for the tuning and validation of the benthic model. The high resolution (~50m) of the hydrodynamic model and its progressive downscaling through nesting with coarser models allows a realistic simulation of circulation, which is crucial for the correct dispersion of aquaculture effluents. As mentioned above, capturing the observed circulation on such a local scale, is rather challenging. Data assimilation would further improve the model skill on such a local scale.

The tool can be used also to examine the potential changes in the environmental status and the impact from aquaculture wastes, under changing climate conditions (i.e., temperature, stratification, etc.), by means of future climate scenario simulations. In this case, the atmospheric forcing is obtained from atmosphere-ocean (climate) model simulations, while open boundary conditions are obtained from a coarser model future climate simulation. The uncertainty of these future climate simulations, however, is relatively high on such local scales, particularly with regard to near surface circulation, given that the usually coarser climate forcing is less relevant at coastal scales. Therefore, these scenario simulations may provide some useful insight on the potential changes of stratification, for example, and its effects on biogeochemistry, but should be considered with caution.

The modelling system can be relatively easily adapted for other areas. The main requirements for the initial model setup are a bathymetry of the area and initial fields for the hydrodynamic (temperature, salinity) and biogeochemical (dissolved inorganic nutrients) models, typically obtained from coarser sub-basin scale models and/or existing climatologies. In addition, fish feed data are also required to calculate the fish farm wastes. The main limitation of the modelling system is that it is computationally very demanding, mainly due to the very high resolution of the near-field model. Overall, the use of AIM as a management tool requires some effort and expertise (scientific for the model output interpretation and technical for the model implementation), but future plans include the dynamic model implementation through a web application that will make this tool more user-friendly.

This project has received funding from the EU H2020 research and innovation programme under Grant Agreement No 678396

6. Mapping regional-scale sustainability for offshore salmon and mussel aquaculture in the North Atlantic and Nordic Seas

6.1. Background

Offshore aquaculture presents a large potential growth area for sustainable exploitation and food provision, avoiding many of the environmental problems and land/water-use conflicts associated with traditional nearshore aquaculture (Benetti et al., 2010; Kapetsky et al., 2013; Jansen et al., 2016; Dale et al., 2017; Gentry et al., 2017; Troell et al., 2017; Oyinlola et al., 2018). Long-term planning and policy development in this regard can benefit from initial broadscale assessments of site suitability, sometimes called “macro-siting” assessments, that can identify regions of interest for further investigation using more focused models and datasets (“micro-siting”, Jansen et al., 2016). Ocean biogeochemical models can enhance macro-siting assessments by providing: 1) more complete datasets than are available from observations, in terms of spatio-temporal coverage and available parameters, and 2) future projections of environmental conditions, allowing us to assess the stability of site suitability under climate change, as is crucial to enable long-term sustainable exploitation. Here we demonstrate the use of a basin-scale ocean biogeochemical model (A20) for macro-siting assessments of offshore salmon and mussel aquaculture in the North Atlantic and Nordic Seas, considering the past 30 years and the future 30 years under the RCP 8.5 climate change scenario.

6.2. Description & limitations of the modelling approach

The A20 model is based on a ROMS ocean model (Shchepetkin and McWilliams, 2005) configured on a 20 km-resolution, pan-Arctic grid developed by the Norwegian Meteorological Institute (Roed et al., 2014). The ecosystem dynamics are based on a version of the ERSEM biogeochemical model (Butenschön et al., 2016) that has been adapted at NIVA for representing high northern latitudes (AERSEM or “Arctic-ERSEM”). The physical and ecosystem models are coupled using the Framework for Aquatic Biogeochemical Models (FABM; Bruggeman and Bolding, 2014). A20 was run in hindcast mode between January 1980 and December 2014, and in projection mode under RCP8.5 from December 2014 through December 2044, with all output saved as weekly averages.

Inputs to the A20 hindcast (1980-2014) included physical initial/boundary conditions from SODA 3.0 (Carton et al., 2000, Carton and Giese, 2008) and biogeochemical initial/boundary conditions from NorESM-OC1.2 (Schwinger et al., 2016). The latter were bias corrected using *in situ* observational data from the World Ocean Database (Boyer et al., 2013), the International Council for the Exploration of the Sea (ICES, Copenhagen, 2013), the Global Ocean Data Analysis Project, version 2 (GLODAPv2, Key et al., 2015; Olsen et al., 2016), the CARINA Iceland and Irminger Sea Time Series version 2 (Olafsson et al., 2009a, 2009b), and various cruise datasets provided by the Shirshov Institute on Oceanology and the Norwegian Environment Agency. Tidal forcing was based on the global ocean tidal model TPXO7.2 from Oregon State University, by imposing surface elevation and corresponding barotropic velocity components at the open boundaries. Atmospheric forcings were based on the ERA-INTERIM archive (Uppala et al. 2005; Reistad et al. 2011) provided by the European Centre for Medium Range Weather Forecast (ECMWF), and CO_2 concentrations from the NOAA Greenhouse

This project has received funding from the EU H2020 research and innovation programme under Grant Agreement No 678396

Gas Marine Boundary Layer Reference (Dlugokency et al., 2015). Freshwater input was mostly from seasonal climatologies, with decadal variability for the major Arctic rivers (Jeffries et al., 2015).

Inputs for the A20 projections (2015-2044) were based on RCP8.5 projections from NORESM (Tjiputra et al., 2016), bias-corrected using the ERA-INTERIM/SODA output for 2006-2015 and the monthly delta change approach of Key and Butenschon (2016). Tidal forcing was used for the hindcast, and riverine forcing was based on a climatology of the hindcast inputs for 2007-2016. The hindcast output for December 2014 was used to set the initial conditions. Source code for creating the forcing files can be found here: https://github.com/trondkr/downscaleA20.

The output for temperature and oxygen in the A20 hindcast and projection runs was bias corrected by first interpolating the hindcast output for 1984-2014 over space and time to the available *in situ* observations (from the above sources), then kernel-smoothing the (model-minus-observations) residuals over (latitude, longitude, depth, month) onto the model grid for each month of the year. The resulting 4D bias field was subsequently interpolated to and subtracted from the A20 hindcasts and projections.

6.3. Model outputs & aquaculture indicators

The A20 model was used to hindcast ocean environmental conditions in the North Atlantic and Nordic Seas over the last 30 years, and to project future conditions over the next 30 years under the RCP8.5 climate change scenario. Model output was stored as weekly averages for physical ocean state and biogeochemical variables and fluxes within the simulated planktonic ecosystem (D6.3, Table A1). In addition, the following "basic sustainability indicators" defined in (M6.3, Table 1) are available as weekly averages: (1) Chlorophyll-a concentration, (2) Phytoplankton carbon, (3) Zooplankton, (4) Surface current velocities, (5) Particulate organic carbon, (9) Dissolved oxygen, (10) pH, (11) Water temperature, (12) Salinity, (15) Ratio dinoflagellates to diatoms, (16) Sum of microplankton + nanoplankton, (17) Phenology of phytoplankton functional types, (20) Ratio silicate-to-nitrogen, (21) Ratio silicate-to-phosphate, (22) Ratio phosphate-to-nitrogen, (23) Upwelling areas, (24) Seabed currents. We also computed the 3D weekly-average horizontal current speed ($(u^2+v^2)^{1/2}$) as an important parameter for aquaculture site selection[4].

Furthermore, we calculated integrated or cumulative indicators (M6.3, Table 2) for Atlantic salmon (*Salmo salar*) and blue mussel (*Mytilus edulis*) aquaculture as described below. These indices should be considered as simple first attempts that illustrate how physical/biogeochemical ocean model output can be exploited for aquaculture planning. See limitations given in Section 6.4.3.

1) *Environmental suitability index for offshore Atlantic salmon farming*.

This considers water depth and other factors (temperature, dissolved oxygen concentration, horizontal current speed; as weekly averages over the surface 0-50 m) and defines an integer value (0 = not suitable, 1 = suitable) for each horizontal grid point and each year. We assume that water depth, estimated using high-resolution bathymetry products (IBCAOv3 (Jakobsson

[4] All output is available on request from Phil Wallhead (pwa@niva.no).

This project has received funding from the EU H2020 research and innovation programme under Grant Agreement No 678396

et al. 2012) and ETOPOv2), must exceed 80 m to allow for maximum 60 m cage depth and minimum 20 m clearance from the bottom (Dale et al., 2017). An upper depth limit is dependent on rapidly-developing mooring techniques/technologies and is difficult to determine at present: Kapetsky et al., (2013) used 100 m, but salmon farms in Norwegian fjords have been successfully moored in water >500 m depth, and an offshore farm has recently been moored down to 300 m. We used 500 m as an upper depth limit for present-day mooring technology. Temperature is required to be within the tolerance range of 3-18 °C for smolts (young) salmon (Norwegian Food Authorities, Dale et al., 2017). Lower limits for the dissolved oxygen concentration are based on experimental results for the limiting oxygen saturation (LOS, Remen et al., 2013), increased by 40% as recommended by Remen et al. (2013) to account for greater feeding and swimming activity in sea cages vs. the experimental conditions (Figure 4.1). This lower limit was modelled as an exponentially increasing function of temperature and was further corrected upwards to account for the presence of a hypothetical fish farm. This latter correction assumed a balance between the net horizontal advection of dissolved oxygen and the consumption of oxygen by fish respiration within the cage (Stigebrandt et al., 2004; Stigebrandt 2011). Here we assumed typical cage dimensions of 40 m width and 30 m depth, and calculated temperature-dependent fish respiration using results from the MOM model (Stigebrandt et al., 2004; Fig. 4) assuming a median fish weight of 1.7 kg and a fish biomass of 667 tonnes per cage. The horizontal current speed was also corrected downwards by 80% to account for the presence of the cage based on results from Aure et al. (2009). An example of the corrected lower limit for the natural (no fish farm) dissolved oxygen concentrations is shown in Fig. 6.1, assuming a natural horizontal current speed of 0.1 m/s. Finally, an upper limit of 0.4 m/s for the fish-farm-corrected current speed was imposed in consideration of the tolerance limits of the smolts (Norwegian Food Authorities, Dale et al., 2017). If any of limits for water depth, temperature, oxygen, or current speed were exceeded for any week of a given year, the site was deemed unsuitable for that year (index value 0), otherwise the site was deemed suitable (index value 1).

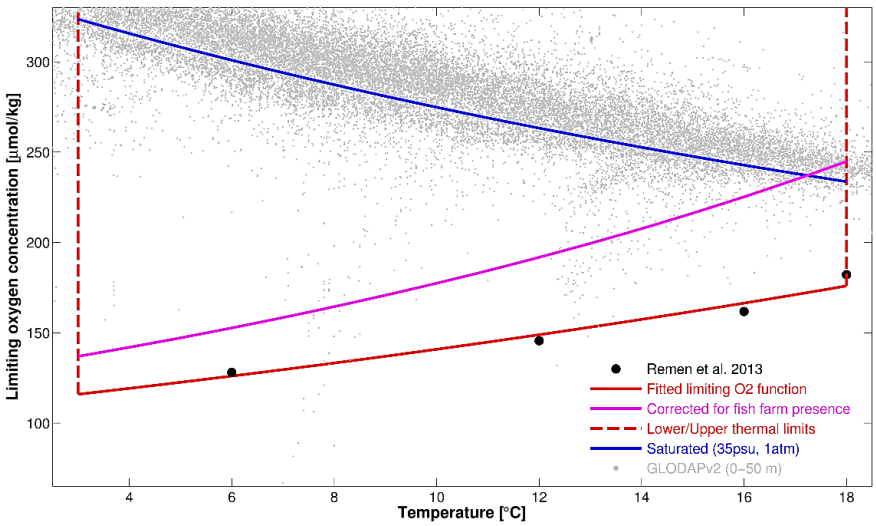

Figure 6.1. An example calculation of limiting oxygen concentrations for Atlantic salmon aquaculture, assuming a minimum weekly-average natural current speed of 0.1 m/s. For comparison we also show the 100%-saturated oxygen concentrations for seawater with salinity 35 psu at 1 atm pressure (blue line) and *in situ* observational data for dissolved oxygen at depths between 0 and 50 m in water columns of depth >25 m (GLODAPv2, grey dots, Olsen et al., 2016; Key et al., 2015).

This project has received funding from the EU H2020 research and innovation programme under Grant Agreement No 678396

2) *Environmental suitability index for offshore blue mussel farming*.

This considers water depth and (temperature, food supply) averaged over years and the surface 0-50 m. Water depth is restricted to between 20 and 500 m, with regard to mooring feasibility, and annual mean temperature is restricted to a "favourable grow-out" range of 2.5–19°C (Kapetsky et al., 2013). Potential food supply to a hypothetical mussel longline is assumed to scale with the horizontal advective flux of particulate organic carbon, given by the product of the mussel-farm-corrected current speed and the ambient POC concentration (e.g. Duarte et al., 2008; Newell and Richardson, 2014). Drag due to friction with the mussel farm is assumed to reduce the current speed by 77.5% (Newell and Richardson, 2014). The food supply is calculated using weekly averages over all depths and is then averaged over 0-50 m and 1 year. A combined suitability index is calculated by multiplying the annual average food supply by the 0-1 indicators for water depth and temperature.

6.4. Assessment of Northern European offshore salmon and mussel aquaculture sustainability under a changing climate scenario

6.4.1 Ecoregions for offshore Atlantic salmon aquaculture

The simple criteria defined in section 6.3 were used to map regions of potential sustainable salmon aquaculture for a given year (e.g. 2014, see Fig. 6.2). Mooring constraints on water depth (80–500 m) restricted production to the deeper parts of the continental shelves, excluding the southern North Sea and English Channel (Fig. 6.2a). For 2014, the annual minimum temperature of 3°C (averaged over 0-50 m and 1 week) imposes a northern border that includes southern Iceland and northern Norway but excludes northern Iceland, the east Greenland coast, and Svalbard (Fig. 6.2b), while the upper limit of 18 °C excludes the southern North Sea and English Channel (Fig. 6.2c). Natural (ambient) dissolved oxygen concentrations are not restrictive (Fig. 6.2d, cf. Fig. 6.1), nor is the upper limit of 0.4 m/s for fish-farm-corrected current speed (Fig. 6.2e). However, surface dissolved oxygen concentrations corrected for the presence of the fish farm may be restrictive in deeper oceanic waters with low current speeds (e.g. over the Lofoten basin, Fig. 6.2f).

This project has received funding from the EU H2020 research and innovation programme under Grant Agreement No 678396

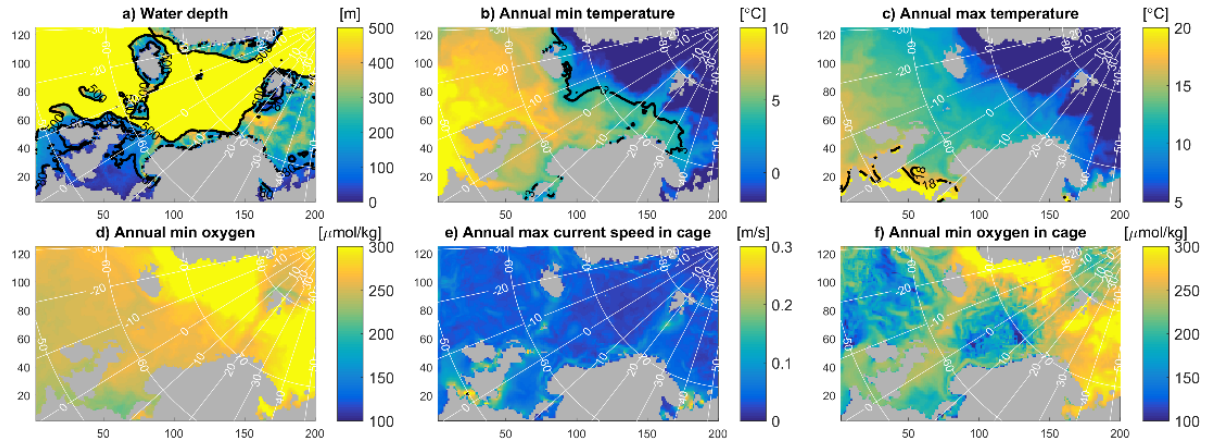

Figure 6.2. An example of sustainability indicators for Atlantic salmon farming in the European sector of the A20 model domain during 2014. All indicators are calculated from weekly and 0-50 m averages (except for water depth). Thick black contour lines show threshold indicator values. White lines show lines of constant latitude/longitude. Axis labels show horizontal coordinates in the A20 domain (1 unit = 20 km).

For the salmon farm analysis, each indicator variable is associated with an integer index value (0 = unsuitable, 1 = suitable) for a given year. By averaging these indices over decades, we can examine the decadal variation in ecoregion extent (see Fig. 6.3). Overall, the total suitable area has been quite stable over the last 3 decades, decreasing by 1% between 1985-1994 and 1995-2004, then increasing by 5% between 1995-2004 and 2005-2014 (Fig. 6.3 d,h,l). These changes appear to be driven mainly by decadal temperature variations, with the northern border extending slightly further into the Barents Sea between 1995-2004 and 2005-2014 (Fig. 6.3 a,e,i).

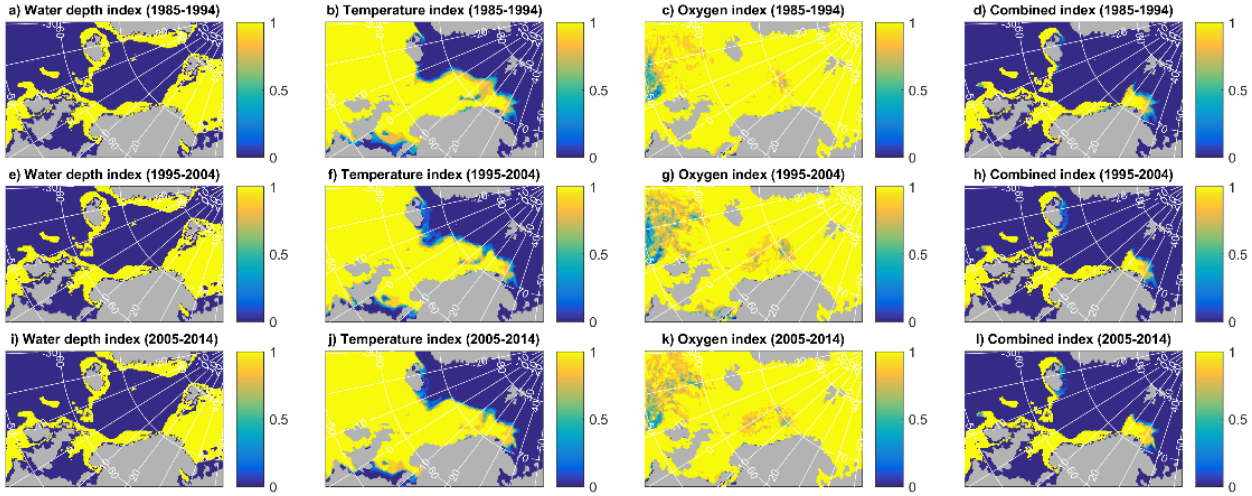

Figure 6.3. Decadal sustainability indices for Atlantic salmon farming in the European sector of the A20 model domain during past decades. Top, middle, and bottom rows show results for decades (1985-1994), (1995-2004), and (2005-2014) respectively. White lines show lines of constant latitude/longitude.

This project has received funding from the EU H2020 research and innovation programme under Grant Agreement No 678396

In the future, under the RCP 8.5 scenario, the A20 projections suggest that regional-scale sustainability will remain stable over the coming 30 years for offshore salmon aquaculture (Figs. 6.4). This stability is enabled by the weak projected trends in annual minimum/maximum (from weekly averages) temperature and dissolved oxygen concentration in the surface waters of the study region over 2015-2044. These trends are on average consistent with the weak corresponding trends in the driving global model (NORESM).

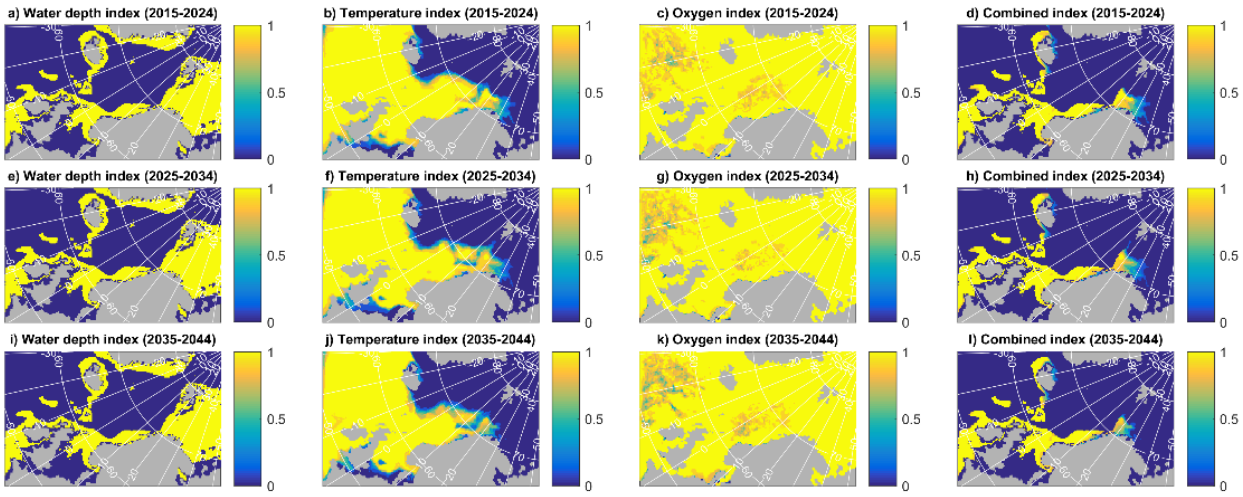

Figure 6.4. Decadal sustainability indices for Atlantic salmon farming in the European sector of the A20 model domain during future decades under the RCP8.5 scenario. Top, middle, and bottom rows show results for decades (2015-2024), (2025-2034), and (2035-2044) respectively. White lines show lines of constant latitude/longitude.

6.4.2 Ecoregions for offshore blue mussel aquaculture

For blue mussel aquaculture, the water depth range (20–500 m) includes almost all of the continental shelf regions in the study region (Fig. 6.5a), and the restrictions of annual mean temperature (2.5–19 °C for the 0-50 m layer) exclude only the eastern Greenland and eastern Svalbard coasts (Fig. 6.5b). Annual mean POC from the model varies rather weakly over the study region (Fig. 6.5c), with lower values in the southern North Sea. Current speed varies strongly over the region (Fig. 6.5d) and appears to be the primary driver of variations in potential food supply (Fig. 6.5e). Combining the water depth and temperature limits with the potential food supply gives an overall sustainability index (Fig. 6.5f) that highlights regions in the German/Southern Bight and the English Channel, and off Brittany, Ireland, Scotland, the northern North Sea, the Faroe Islands, Iceland, the Danish and Norwegian coast (especially in the south), and parts of the Barents Sea and western Svalbard shelf. This pattern has been quite stable over recent decades, extending slightly northwards into the Barents Sea with warming between 2000 and 2010 (Fig. 6.6).

This project has received funding from the EU H2020 research and innovation programme under Grant Agreement No 678396

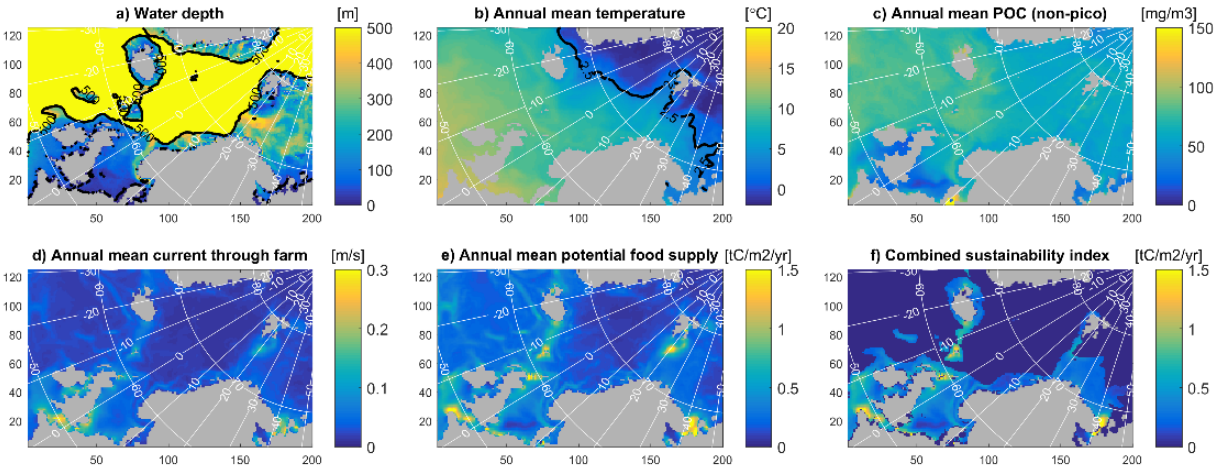

Figure 6.5. An example of sustainability indicators for blue mussel farming in the European sector of the A20 model domain during 2014. All indicators are calculated from annual and 0-50 m averages (except for water depth). Thick black contour lines show threshold indicator values. White lines show lines of constant latitude/longitude. Axis labels show horizontal coordinates in the A20 domain (1 unit = 20 km).

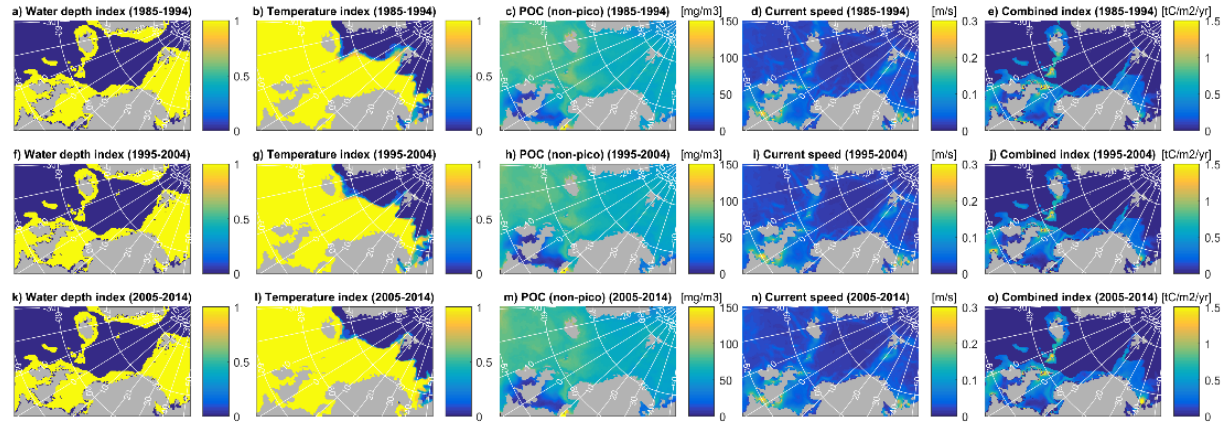

Figure 6.6. Decadal sustainability indices for blue mussel farming in the European sector of the A20 model domain in past decades. Top, middle, and bottom rows show results for decades (1985-1994), (1995-2004), and (2005-2014) respectively. White lines show lines of constant latitude/longitude.

In the future, under the RCP8.5 scenario, the A20 projections suggest that regional-scale sustainability will also remain stable over the coming 30 years for offshore mussel aquaculture (Fig. 6.7). Again, this projected stability is due to weak projected trends over the next 30 years, in this case for annual mean temperature and POC in the surface waters.

This project has received funding from the EU H2020 research and innovation programme under Grant Agreement No 678396

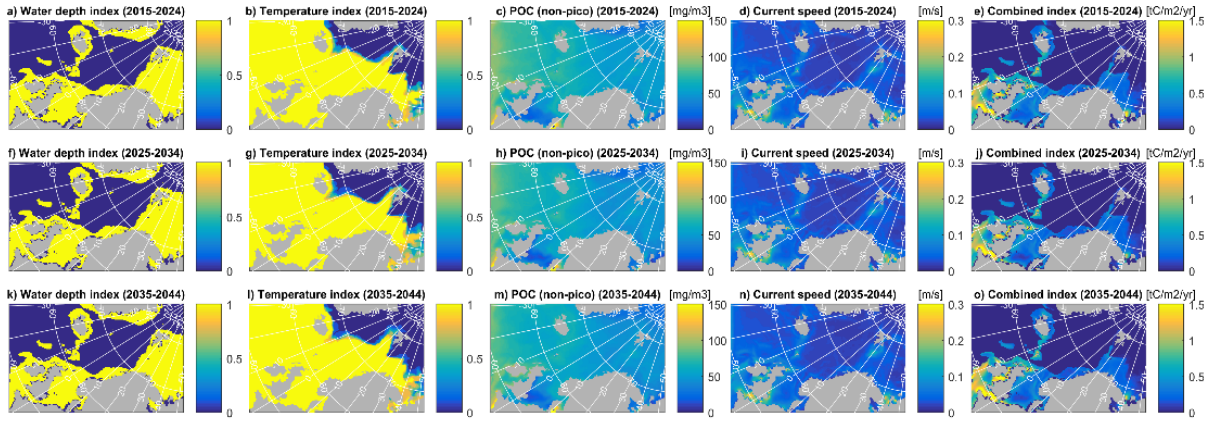

Figure 6.7. Decadal sustainability indices for blue mussel farming in the European sector of the A20 model domain in the future under the RCP8.5 scenario. Top, middle, and bottom rows show results for decades (2015-2024), (2025-2034), and (2035-2044) respectively. White lines show lines of constant latitude/longitude.

6.4.3 Caveats and limitations

It must be emphasized that the indicators described above are rather simple and only partially determine the suitability of a given site for offshore salmon or mussel aquaculture. Other factors include administrative/legal constraints (existing aquaculture, marine protected areas, coastal waterways, offshore windfarms), logistical constraints on distance from land (or manned station/rig for supply and servicing of the farm), and safety/technological constraints (e.g., significant wave height and frequency of navigable ocean conditions) (Dale et al., 2017). Also, there are limitations of the present (A20) model output used to calculate the indicators, notably the 20-km spatial resolution which is not sufficient to resolve ocean eddies at moderate/high latitudes (e.g., Holt et al., 2014), hence the impact of eddies on average current speeds and biogeochemical production (e.g., POC production and subsequent oxygen consumption) is not fully accounted for. Also, the simple nature of the indicators likely misses some important interaction effects, e.g. mussel production may require higher food supply at lower temperature. Nevertheless, such analyses appear to be a useful first step for highlighting broad-scale potential areas of future blue growth and may subsequently help to guide and focus more refined models and analyses at smaller spatial scales.

6.4.4 Conclusions

This case study demonstrates how basin-scale regional downscaling models can be applied to explore the sustainability of offshore salmon and mussel aquaculture. Our results suggest that large regions of the European/Nordic shelf seas could be utilized for offshore aquaculture, if logistical and administrative constraints can be overcome. Our future projections based on a single climate model and a pessimistic (high-emissions) climate change scenario suggested that the potential for sustainable aquaculture will not change significantly over the next 30 years (based on environmental constraints) although a more rigorous analysis using an ensemble of climate models, and possibly higher-resolution climate models, should be employed to provide uncertainty estimates for these projections.

This project has received funding from the EU H2020 research and innovation programme under Grant Agreement No 678396

This type of large-scale “macro-siting” approach is useful for identifying broad regions of interest that can be further investigated using more focused models with higher spatial and process resolution but more limited geographic scope (“micro-siting”, Jansen et al., 2016). It is therefore more likely useful for strategic, long-term planning of aquaculture and policy development (e.g. expansion into offshore areas as potential regions of future blue growth and sustainable exploitation).

6.4.4 Broader applicability

This case study demonstrates, within the caveats and limitations given, the potential utility of 3D regional ocean biogeochemical models as tools to guide large-scale and long-term aquacultural planning and policy development. While similar broad-scale “macro-siting” analyses have been performed using only observational data (e.g. Kapetsky et al., 2013; Gentry et al., 2017), the use of an ocean biogeochemical model (such as the A20 ROMS-ERSEM coupled models used herein) has two major potential benefits: 1) The models can provide complete time series of variability at all depths and horizontal locations, not subject to gaps or sampling biases, and may thus provide more robust estimates of e.g. annual minimum oxygen concentrations; 2) The models can provide future projections, thus allowing us to investigate how different scenarios of anthropogenic change may impact conditions at a regional scale, allowing policy-makers to identify potential zones that could be used for aquaculture into the future, subject to local-scale assessment.

This project has received funding from the EU H2020 research and innovation programme under Grant Agreement No 678396

7. Conclusions

Earth Observation (EO)- and modelling-generated biogeochemical variables crucial to the success and sustainability of the aquaculture industry have been used here to establish and demonstrate a range of far-field aquaculture indicators for Europe. Some of these variables (e.g., water temperature, dissolved oxygen concentration, current speed) are used by applying thresholding or similar approaches that make use of known tolerance ranges or biological cues from the literature to identify areas where certain aquaculture sectors would be possible or not possible. In other instances, these model outputs are used in further carrying capacity or organismal growth modelling, which are then transformed into environmental or industry indicators to further constrain which areas may be better suited within the identified tolerance range. The ensemble of approaches presented demonstrate the versatility and utility of EO and modelled physical and biogeochemical data to aquaculture planning and policy generally, with particular approaches and related indicators to be selected depending on the given need.

Use of spatiotemporal data in developing such indicators has the advantage of full coverage for large areas, particularly compared with conventional *in situ* datasets, as well as the possibility to consider different periods in the case of model outputs. In all of the approaches presented here, the use of climatologies, taken to be largely representative conditions of the time period considered (e.g., a mean year of twenty years of modelled output), is expected to provide more reliable information for the comparison of different periods. The exploration of several possible future climate scenarios, given the high degree of related uncertainty and the effect thereof on ocean biogeochemistry and aquaculture, is incorporated into several of the proposed indicators, and the stability of a given indicator over time and in light of climate change is itself considered. Some approaches also applied different management scenarios, and were therefore able to highlight and discuss the respective degree of influence of modelled climate change and management practices on the respective aquaculture sector.

Although *TAPAS* work at the near-field scale, corresponding to farms and water bodies such as bays, has revealed high spatial variability of aquaculture potential (see *TAPAS* deliverable 5.5), the use of far-field biogeochemical satellite observation and modelling data is suggested to inform higher-level planning and policy development. Large-scale zoning, as presented here, has been demonstrated to highlight broad areas of particular interest for such purposes, which can be targeted for more detailed or high-resolution investigation for farm-scale siting. All of the approaches presented here consider the influence of multiple variables on aquaculture potential and sustainability, but they also acknowledge that there are many other factors that underly whether aquaculture will be possible at a certain location or not and, within this, where aquaculture would be best situated. Such factors include conflicting fisheries, military, or tourism uses and the presence of necessary infrastructure (e.g., ports within a reasonable distance), among many others. Although the consideration of these and other influencing factors are beyond the scope of the present work, which is to present and demonstrate the application of a suite of aquaculture indicators, large-scale zoning using our indicators would be further enhanced by including them in full spatial multi-criteria evaluation for marine spatial planning.

This project has received funding from the EU H2020 research and innovation programme under Grant Agreement No 678396

8. References

AFNOR, 1985. Norme française huîtres creuses. Dénomination et classification. NF V 45-056, 5p.

Aure, J., Vigen, J., Oppedal, F. 2009. Hva bestemmer vannutskiftning og oksygenforhold i oppdrettsmerder? Kyst og Hav bruk 2009, Havforskningsinstituttet, Bergen, 169−171.

Baretta, J. W., Ebenhöh, W., Ruardij, P. 1995. The European regional seas ecosystem model, a complex marine ecosystem model. *Netherlands Journal of Sea Research*, 33(3): 233–246.

Barillé L., Prou J., Héral M. & S. Bougrier, 1993. No influence of food quality, but ration-dependent retention efficiencies in the Japanese oyster *Crassostrea gigas*. *Journal of Experimental Marine Biology and Ecology,* 171, pp. 91-106.

Barton, A., Hales, B., Waldbusser, G. G., Langdon, C., Feely, R. A. 2012. The Pacific oyster, *Crassostrea gigas*, shows negative correlation to naturally elevated carbon dioxide levels: Implications for near-term ocean acidification effects. *Limnology and Oceanography*, 57(3): 698-710.

Bayne, B. 2017. Biology of oysters. Elsevier Academic Press, *Development in Aquaculture* and *Fisheries Science Volume 41*, 843 ppBenetti D. D., Benetti, G. I., Rivera, J. A., Sardenberg, B., O'Hanlon, B. 2010. Site selection criteria for open ocean aquaculture. *Marine Technology Society Journal*, 44(3): 22-35.

Bernard, I., de Kermoysan, G., Pouvreau, S. 2011. Effect of phytoplankton and temperature on the reproduction of the Pacific oyster *Crassostrea gigas*: Investigation through DEB theory. *Journal of Sea Research*, 66: 349–360.

Boyer, T. P., Antonov, J. I., Baranova, O. K., Coleman, C., Garcia, H. E., Grodsky, A., Johnson, D. R., Locarnini, R. A., Mishonov, A. V., O'Brien, T. D., Paver, C. R. 2013. World Ocean Database 2013, Sydney Levitus, Ed.; Alexey Mishonoc, Tech. Ed., NOAA Atlas(72), 209 pp, doi:http://doi.org/10.7289/V5NZ85MT.

Broell, F., McCain, J., Taggart, C. 2017. Thermal time explains size-at-age variation in molluscs. *Marine Ecology Progress Series*, 573: 157–165.

Bruggeman J., Bolding, K. 2014. A general framework for aquatic biogeochemical models. *Environmental Modelling & Software*, 61: 249–265.

Buck, B. H., Langan, R. 2017. Aquaculture Perspective of Multi-Use Sites in the Open Ocean. SpringerOpen.

Butenschön, M., Clark, J., Aldridge, J. N., Allen, J. I., Artioli, Y., Blackford, J., Bruggeman, J., Cazenave, P., Ciavatta, S., Kay, S., Lessin, G., van Leeuwen, S., van der Molen, J., de Mora, L., Polimene, L., Sailley, S., Stephens, N., Torres, R. 2016. ERSEM 15.06: a generic model for marine biogeochemistry and the ecosystem dynamics of the lower trophic levels. *Geoscientific Model Development*, 9: 1293–1339.

Carton, J. A., Chepurin, G., Cao, X., Giese, B. 2000. A Simple Ocean Data Assimilation Analysis of the Global Upper Ocean 1950–95. Part I: Methodology. *Journal of Physical Oceanography*, 30: 294–309.

Carton, J. A., Giese, B. 2008. A Reanalysis of Ocean Climate Using Simple Ocean Data Assimilation (SODA). *Monthly Weather Review*, 136: 2999-3017.

Ciavatta, S., Kay, S., Saux-Picart, S., Butenschön, M., Allen, J. I. 2016. Decadal reanalysis of biogeochemical indicators and fluxes in the North West European shelf-sea ecosystem. *Journal of Geophysical Research: Oceans*, 121(3): 1824-1845.

Dale, T., Cusack, C., Ruiz, M. 2017. Aquaculture site selection Report. AtlantOS Deliverable, D8.2 . AtlantOS, 39 pp. DOI 10.3289/AtlantOS_D8.2.

Dlugokency, E. J., Masarie, K. A., Lang, P. M., Tans, P. P. 2015. NOAA Greenhouse Gas Reference from Atmospheric Carbon Dioxide Dry Air Mole Fractions from the NOAA

This project has received funding from the EU H2020 research and innovation programme under Grant Agreement No 678396

ESRL Carbon Cycle Cooperative Global Air Sampling Network. Data Path: ftp://aftp.cmdl.noaa.gov/data/trace_gases/co2/flask/surface/.

Donnelly, C., Andersson, J. C., Arheimer, B. 2016. Using flow signatures and catchment similarities to evaluate the E-HYPE multi-basin model across Europe. *Hydrological Sciences Journal*, 61(2): DOI:10.1080/02626667.2015.1027710.

Duarte, P., Labarta, U., Fernandez-Reiriz, M. J. 2008. Modelling local food depletion effects in mussel rafts of Galician Rias. *Aquaculture*, 274:300–312.

Falconer, L., Palmer, S., Barillé, L., Gernez, P., Torres, R., Cazenave, P., Artioli, Y., Hawkins, A., Bedington, M., Simis, S., Miller, P., Dabrowski, T., Othmani, A., Mamoutos, I. 2019. Improved modelling approaches for shellfish production in coastal, intertidal and offshore environments. TAPAS project Deliverable 5.5 report. 58pp.

FAO. 2018. The State of World Fisheries and Aquaculture 2018 - Meeting the sustainable development goals. Rome. Licence: CC BY-NC-SA 3.0 IGO.

Gattuso, J. P., Magnan, A., Billé, R., Cheung, W. W., Howes, E. L., Joos, F., Allemand, D., Bopp, L., Cooley, S.R., Eakin, C.M., Hoegh-Guldberg, O. 2015. Contrasting futures for ocean and society from different anthropogenic CO2 emissions scenarios. *Science*, 349(6243): aac4722.

Gentry R. R., Froehlich, H. E., Grimm, D., Kareiva, P., Parke, M., Rust, M., Gaines, S. D., Halpern, B.S. 2017. Mapping the global potential for marine aquaculture. *Nature Ecology & Evolution*, 1(9):1317-1324.

Gosling, E. Bivalve Molluscs: Biology, Ecology and Culture; Wiley-Blackwel: Hoboken, NJ, USA, 2003.

Han, B., Loisel, H., Vantrepotte, V., Mériaux, X., Bryère, P., Ouillon, S., Dessailly, D., Xing, Q., Zhu, J. 2016. Development of a Semi-Analytical Algorithm for the Retrieval of Suspended Particulate Matter from Remote Sensing over Clear to Very Turbid Waters. *Remote Sensing*, 8(3): 211. https://doi.org/10.3390/rs8030211.

Herbert, R. J. H., Humphreys, J., Davies, C. J., Roberts, C., Fletcher, S., Crowe, T. P. 2016. Ecological impacts of non-native Pacific oysters (*Crassostrea gigas*) and management measures for protected areas in Europe. *Biodiversity and Conservation*, 25(14): 2835–2865.

Hofherr, J., Natale, F., Trujillo, P., 2015. Is lack of space a limiting factor for the development of aquaculture in EU coastal areas? *Ocean & Coastal Management*, 116: 27-36.

Holm, P., Buck, B. H., Langan, R. 2017. Introduction: New Approaches to Sustainable Offshore Food Production and the Development of Offshore Platforms. In: Buck B., Langan R. (eds) Aquaculture Perspective of Multi-Use Sites in the Open Ocean. SpringerOpen.

Holt, J. T., James, I. D. 2001. An s coordinate density evolving model of the northwest European continental shelf 1, Model description and density structure. *Journal of Geophysical Research*, 106 : 14015–14034.

Holt, J., Allen, J. I., Anderson, T. R., Brewin, R., Butenschön, M., Harle, J., Huse, G., Lehodey, P., Lindemann, C., Memery, L., Salihoglu, B. 2014. Challenges in integrative approaches to modelling the marine ecosystems of the North Atlantic: Physics to fish and coasts to ocean. *Progress in Oceanography*, 129(PB): 285–313.

IPCC. 2019. IPCC special report on the ocean and cryosphere in a changing climate. Chapter 5: Changing ocean, marine ecosystems, and dependent communities. 198 pp.

Jakobsson, M., Mayer, L., Coakley, B., Dowdeswell, J. A., Forbes, S., Fridman, B., Hodnesdal, H., Noormets, R., Pedersen, R., Rebesco, M., Schenke, H. W. 2012. The International Bathymetric Chart of the Arctic Ocean (IBCAO) version 3.0. *Geophysical Research Letters*, 39: L12609.

Kapetsky, J. M., Aguilar-Manjarrez, J., Jenness, J. 2013. A global assessment of potential for offshore mariculture development from a spatial perspective. FAO Fisheries and Aquaculture Technical Paper No. 549. Rome, FAO. 181 pp.

This project has received funding from the EU H2020 research and innovation programme under Grant Agreement No 678396

Kay, S., Butenschon, M. 2018. Projections of change in key ecosystem indicators for planning and management of marine protected areas: An example study for European seas. *Estuarine, Coastal and Shelf Science*, 201: 172-184.

Key, R. M., Olsen, A., van Heuven, S., Lauvset, S. K., Velo, A., Lin, X., Schirnick, C., Kozyr, A., Tanhua, T., Hoppema, M., Jutterström, S. 2015. Global Ocean Data Analysis Project, Version 2 (GLODAPv2), OakRidge, Tennessee.

Kooijman, S. A. L. M. 2010. Dynamic energy budget theory for metabolic organisation. Cambridge University Press.

Kroeker, K. J., Kordas, R .L., Crim, R. N., Singh, G. G. 2010. Meta-analysis reveals negative yet variable effects of ocean acidification on marine organisms. *Ecology letters*, 13(11): 1419-1434.

Kurekin, A. A., Miller, P. I., Van der Woerd, H. J. 2014. Satellite discrimination of Karenia mikimotoi and Phaeocystis harmful algal blooms in European coastal waters: Merged classification of ocean colour data. *Harmful Algae*, 31: 163-176.

Jackson, T., Sathyendranath, S., Mélin, F. 2017. An improved optical classification scheme for the Ocean Colour Essential Climate Variable and its applications. *Remote Sensing of Environment*, 203: 152-161.

Jansen, H. M., Van Den Burg, S., Bolman, B., Jak, R. G., Kamermans, P., Poelman, M., Stuiver, M. 2016. The feasibility of offshore aquaculture and its potential for multi-use in the North Sea. *Aquaculture International*, 24(3): 735-756.

Jeffries, M. O., Richter-Menge, J., Overland, J. E., Eds., 2015. Arctic Report Card 2015, http://www.arctic.noaa.gov/Report-Card.

Meaden, G. J., Aguilar-Manjarrez, J. 2013. Advances in geographic information systems and remote sensing for fisheries and aquaculture. FAO Fisheries and Aquaculture Technical Paper, (552), p.I.

Moore, T. S., Dowell, M. D., Bradt, S., Verdu, A. R. 2014. An optical water type framework for selecting and blending retrievals from bio-optical algorithms in lakes and coastal waters. *Remote Sensing of Environment*, 143: 97-111.

Moss, R. H., Edmonds, J. A., Hibbard, K. A., Manning, M. R., Rose, S. K., Van Vuuren, D. P., Carter, T. R., Emori, S., Kainuma, M., Kram, T., Meehl, G. A. 2010. The next generation of scenarios for climate change research and assessment. *Nature*, 463(7282): 747.

Nell, J.A., Holliday, J.E., 1988. Effect of salinity on the growth and survival of Sydney rock oyster (*Saccostrea commercialis*) and Pacific oyster (*Crassostrea gigas*) larvae and spat. *Aquaculture*, 68: 39-44.

Newell, C. R., Richardson, J. 2014. The effects of ambient and aquaculture structure hydrodynamics on the food supply and demand of mussel rafts. *Journal of Shellfish Research*, 33(1): 257–272.

Olafsson, J., Olafsdottir, S. R., Benoit-Cattin, A., Danielsen, M., Arnarson, T. S., Takahashi, T. 2009a. Rate of Iceland Sea acidification from time series measurements. *Biogeosciences*, 6(11), 2661-2668.

Olafsson, J., Olafsdottir, S. R., Benoit-Cattin, A., Takahashi, T. 2009b. The Irminger Sea and the Iceland Sea time series measurements of sea water carbon and nutrient chemistry 1983–2006. *Earth System Science Data*, 2(1): 477–492.

Olsen, A., Key, R. M., Van Heuven, S., Lauvset, S. K., Velo, A., Lin, X. 2016. An internally consistent data product for the world ocean: the Global Ocean Data Analysis Project, version 2 (GLODAPv2), doi:10.5194/essd-2015-42.

Oyinlola, M. A., Reygondeau, G., Wabnitz, C. C. C., Troell, M., Cheung, W. W. L. 2018. Global estimation of areas with suitable environmental conditions for mariculture species. *PLoS ONE*, 13 (1): e0191086.

This project has received funding from the EU H2020 research and innovation programme under Grant Agreement No 678396

Palmer, S. C. J., Gernez, P., Thomas, Y., Simis, S., Miller, P., Glize, P., Barillé, L. 2019. Remote sensing-driven Pacific oyster (*Crassostrea gigas*) growth modeling to inform offshore aquaculture site selection. Submitted to Frontiers in Marine Science, 25/09/2019 (submission number: 500467).

Petihakis, G., Tsiaras, K., Traintafyllou, G., Korres, Tsagaraki, T. M., Tsapakis, M., Vavillis, P., Pollani, A., Frangoulis, C. 2012. Application of a complex ecosystem model to evaluate effects of finfish culture in Pagasitikos Gulf, Greece. *Journal of Marine Systems*, 94: S65-S77.

Pogoda, B., Buck, B. H., Hagen, W. 2011. Growth performance and condition of oysters (*Crassostrea gigas* and *Ostrea edulis*) farmed in an offshore environment (North Sea, Germany). *Aquaculture*, 319(3-4): 484-492.

Pouvreau, S., Bourles, Y., Lefebvre, S., Gangnery, A., Alunno-Bruscia, M. 2006. Application of a dynamic energy budget model to the Pacific oyster, *Crassostrea gigas*, reared under various environmental conditions. *Journal of Sea Research*, 56: 156–167.

Primpas, I., Tsirtsis, G., Karydis, M., Kokkoris, G. D. 2010. Principal component analysis: Development of a multivariate index for assessing eutrophication according to the European water framework directive. *Ecological Indicators*, 10: 178–183.

Reistad, M., Breivik, Ø., Haakenstad, H., Aarnes, O. J., Furevik, B. R., Bidlot, J. R. 2011. A high-resolution hindcast of wind and waves for the North Sea, the Norwegian Sea, and the Barents Sea. *Journal of Geophysical Research: Oceans,* 116(C5).

Remen, M., Oppedal, F., Imsland, A. K., Olsen, R. E., Torgersen, T. 2013. Hypoxia tolerance thresholds for post-smolt Atlantic salmon: dependency of temperature and hypoxia acclimation. *Aquaculture*, 416: 41–47.

Roed et al., 2014. Evaluation of the BaSIC20 long term hindcast results. BaSIC Technical Report 3, Norwegian Meterological Institute.

Sanchez-Jerez P., Karakassis I., Massa F., Fezzardi, D. Aguilar-Manjarrez, J., Soto, D., Chapela, R., Ávila, P., Macías, J. C., Tomassetti, P., Marino, G. 2016. Aquaculture's struggle for space: the need for coastal spatial planning and the potential benefits of Allocated Zones for Aquaculture (AZAs) to avoid conflict and promote sustainability. *Aquaculture Environment Interactions*, 8:41-54.

Schwinger, J., Goris, N., Tjiputra, J. F., Kriest, I., Bentsen, M., Bethke, I., Ilicak, M., Assmann, K. M., Heinze, C. 2016. Evaluation of NorESM-OC (versions 1 and 1.2), the ocean carboncycle stand-alone configuration of the Norwegian Earth System Model (NorESM1), *Geoscientific Model Development*, 9: 2589-2622.

Shchepetkin, A. F., McWilliams, J. C. 2005. The Regional Ocean Modeling System (ROMS): A split-explicit, free-surface, topography-following coordinate ocean model. *Ocean Modelling*, 9: 347–404.

Shelmerdine, R.L., Mouat, B. and Shucksmith, R.J., 2017. The most northerly record of feral Pacific oyster *Crassostrea gigas* (Thunberg, 1793) in the British Isles. *BioInvasions Records*, 6: 57-60.

Spyrakos, E., O'Donnell, R., Hunter, P. D., Miller, C., Scott, M., Simis, S. G., Neil, C., Barbosa, C. C., Binding, C. E., Bradt, S., Bresciani, M. (2018). Optical types of inland and coastal waters. *Limnology and Oceanography*, 63(2): 846-870.

STECF. 2018. Scientific, Technical and Economic Committee for Fisheries (STECF) – Economic report of the EU Aquaculture sector (STECF-18-19). Publications office of the European Union, Luxembourg, 2018 JRC114801.

Stigebrandt, A., Aure, J., Ervik, A., Hansen, P.K. 2004. Regulating the local environmental impact of intensive marine fsh farming. III. A model for estimation of the holding capacity in the MOM system (Modelling – Ongrowing Fish Farm – Monitoring). *Aquaculture*, 234: 239-261.

Stigebrandt, A. 2011. Carrying capacity: general principles of model construction. *Aquaculture Research*, 42: 41-50.

This project has received funding from the EU H2020 research and innovation programme under Grant Agreement No 678396

Syvret, M., Fitzgerald, A., Hoare, P. 2008. Development of a Pacific oyster aquaculture protocol for the UK— Technical Report FIFG project no: 07/Eng/46/04. Report for the Sea Fish Industry Authority.

Thomas, Y., Pouvreau, S., Alunno-Bruscia, M., Barillé, L., Gohin, F., Bryère, P., Gernez, P. 2016. Global change and climate-driven invasion of the Pacific oyster (*Crassostrea gigas*) along European coasts: a bioenergetics modelling approach. *Journal of Biogeography*, 43(3): 568-579.

Tjiputra, J. F., Grini, A., Lee, H. 2016. Impact of idealized future stratospheric aerosol injection on the large-scale ocean and land carbon cycles. *Journal of Geophysical Research: Biogeosciences*, 121: 2–27.

Troell, M., Jonell, M., Henriksson, P. J. G. 2017. Ocean space for seafood. *Nature Ecology & Evolution*, 1(9): 1224-5.

Tsagaraki, T. M., Petihakis, G., Tsiaras, K., Triantafyllou, G., Tsapakis, M., Korres, G., Kakagiannis, G., Frangoulis, C., Karakassis, I. 2011. Beyond the cage: ecosystem modelling for impact evaluation in aquaculture. *Ecological Modelling*, 222(14): 2512-2523.

Tsapakis, M., Pitta, P., Karakassis, I., 2006. Nutrients and fine particulate matter released from sea bass (Dicentrachus labrax) farming. *Aquatic Living Resources*, 19: 69–75.

Uppala, S. M., KÅllberg, P. W., Simmons, A. J., Andrae, U., Bechtold, V. D. C., Fiorino, M., Gibson, J. K., Haseler, J., Hernandez, A., Kelly, G. A., Li, X., Onogi, K., Saarinen, S., Sokka, N., Allan, R. P., Andersson, E., Arpe, K., Balmaseda, M. A., Beljaars, A. C. M., Berg, L. V. D., Bidlot, J., Bormann, N., Caires, S., Chevallier, F., Dethof, A., Dragosavac, M., Fisher, M., Fuentes, M., Hagemann, S., Hólm, E., Hoskins, B. J., Isaksen, L., Janssen, P. A. E. M., Jenne, R., Mcnally, A. P., Mahfouf, J.-F., Morcrette, J.-J., Rayner, N. A., Saunders, R. W., Simon, P., Sterl, A., Trenberth, K. E., Untch, A., Vasiljevic, D., Viterbo, P., Woollen, J. 2005. The ERA-40 re-analysis. *Quarterly Journal of the Royal Meteorological Society*, 131: 2961–3012.

Van Vuuren, D. P., Edmonds, J., Kainuma, M., Riahi, K., Thomson, A., Hibbard, K., Hurtt, G. C., Kram, T., Krey, V., Lamarque, J. F., Masui, T. 2011. The representative concentration pathways: an overview. *Climatic Change*, 109(1-2): 5.

This project has received funding from the EU H2020 research and innovation programme under Grant Agreement No 678396

[End page leave blank]

This project has received funding from the EU H2020 research and innovation programme under Grant Agreement No 678396